

**DESIGN AND OFF-DESIGN
PERFORMANCE ANALYSIS OF A ZIGZAG
CHANNELED PRECOOLER FOR SCO₂
RECOMPRESSION CYCLE INTEGRATED
WITH CSP**

Md. Maruf Ahmed, 170011030

Submitted in Partial
Fulfillment of the
Requirements
for the Degree of

Bachelor of Science in Mechanical Engineering


**DEPARTMENT OF MECHANICAL AND PRODUCTION
ENGINEERING**

May (2022)

CERTIFICATE OF RESEARCH

This thesis titled "DESIGN AND OFF-DESIGN PERFORMANCE ANALYSIS OF A ZIGZAG CHANNЕLED PRECOOLER FOR SCO2 RECOMPRESSION CYCLE INTEGRATED WITH CSP" submitted by MD. MARUF AHMED (170011030) has been accepted as satisfactory in partial fulfillment of the requirement for the Degree of Bachelor of Science in Mechanical Engineering.

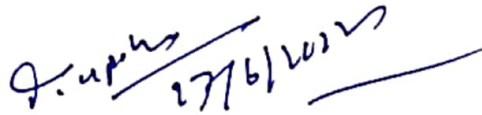
Supervisor


27.06.22

Dr. Mohammad Monjurul Ehsan

Associate Professor

Head of the Department


27/6/2022

Dr. Md. Anayet Ullah Patwari

Professor

*Department of Mechanical and Production Engineering
(MPE) Islamic University of Technology (IUT)*

DECLARATION

I hereby declare that this thesis entitled "Design and Off-design Performance Analysis of a Zigzag Channeled Pre-cooler for sCO₂ Recompression cycle integrated with CSP" is an authentic report of study carried out as requirement for the award of degree B.Sc. (Mechanical Engineering) at Islamic University of Technology, Gazipur, Dhaka, under the supervision of Dr. Mohammad Monjurul Ehsan, Associate Professor, MPE, IUT in the year 2022

The matter embodied in this thesis has not been submitted in part or full to any other institute for award of any degree.

Maruf, 27.06.22

Student Name: Md. Maruf Ahmed

Student ID: 170011030

ACKNOWLEDGEMENT

In the Name of Allah, the Most Beneficent, the Most Merciful.

First of all, I am grateful to ALLAH (SWT), the most benevolent and kind to provide me the strength and ability to write this dissertation. I want to thank my project supervisor, Dr. Mohammad Monjurul Ehsan, for his strong and patient support through unpredictable problems during the project and his precious advice when I faced difficulties. His generosity, kindness and strong supervision during work made me feel less stressed in confronting unexpected troubles and be more productive in my personal life.

In the next step, I would like express my deep acknowledgment to my father and mother for their continued support and dedication towards my higher study.

ABSTRACT

The design and performance analysis of Printed Circuit Heat Exchanger (PCHE) as pre-cooler is being recent research trend as the researches on recuperator has already been saturated. The improbable fluctuating properties of sCO₂ near the critical region makes it arduous to design a component that runs under the critical region. However, the high heat transfer coefficient at near critical region is advantageous in increasing the second law efficiency of the power cycle and reducing the size of cycle components, making it cost effective. In this study an iterative nodal approach is implemented to develop a design code in Python language for the design of zigzag channeled PCHE as the pre-cooler for sCO₂ recompression cycle integrated with Concentrated Solar Power technology. For the real gas properties (RGP) of sCO₂ CoolProp is used. The performance study done under different sCO₂ inlet pressure and different water inlet temperature suggest the heat transfer rate can be enhanced by lowering the water inlet temperature and sCO₂ pressure down to 7.5MPa. The result also shows the pressure drop on sCO₂ side decreases upon increasing these parameters. The outcomes derived from this work can be used to design and develop more advanced PCHEs for pre-cooler application for wide range of Cooling-loads.

Keywords: PCHE, Zigzag, sCO₂, Recompression , CSP

TABLE OF CONTENTS

Acknowledgement	i
Abstract	ii
Table of Contents	iii
List of Figures	v
List of Tables	vi
Nomenclature	vii
Subscripts	viii
Greek	viii
Abbreviations	ix
1 INTRODUCTION	1
1.1 Background	1
1.2 Problem Statement	2
1.3 Methodology of the study	4
1.4 Arrangement	4
1.5 Limitations	4
2 LITERATURE REVIEW	5
2.1 Review of S-CO ₂ Recompression cycle	5
2.2 Review on PCHE	6
3 RESEARCH DESIGN	11
3.1 Introduction	11
3.2 sCO ₂ Recompression cycle Layout	12
3.3 Physical Model	14
3.3.1 Equations for Defining Channel Geometry	19
3.3.2 PCHE Combination	21
3.4 Mathematical Model	22
3.4.1 Assumptions	22
3.4.2 Boundary Conditions	22
3.4.3 Nodal Approach	23
3.5 CODE VALIDATION	30
4 DATA GENERATION / COLLECTION, ANALYSIS AND DISCUSSION ...	31
4.1 Temperature Profiles	31
4.2 Heat Transfer Characteristics	32
4.2.1 Uncertainties	33
4.3 Pressure Drop Characteristics	34

4.4	Off Design	37
4.4.1	Effect of sCO ₂ Inlet Pressure	37
4.4.2	Effect of Water Inlet Temperature	40
5	CONCLUSION AND RECOMMENDATION	45
	References	46

LIST OF FIGURES

<i>Figure 1: Abrupt change of Carbon dioxide properties(RGP)extracted from CoolProp near the pseudo-critical temperature at Pre-cooler design operating Pressure(8MPa)</i>	10
<i>Figure 2: Size comparison of PCHE to STHE</i>	11
<i>Figure 3: sCO2 Recompression integrated with CSP</i>	18
<i>Figure 4: Split view of PCHE (Courtesy MEGGiT("Printed Circuit Heat Exchangers - Meggitt" n.d.))</i>	21
<i>Figure 5:The 3D view for channel configuration and nozzle flanges</i>	21
<i>Figure 6: Zigzag Channel Geometry</i>	22
<i>Figure 7: Characteristics Length of Hot and Cold Channels</i>	23
<i>Figure 8: PCHE module combination for required Heat Rejection</i>	27
<i>Figure 9: Nodal Approach across the length.</i>	31
<i>Figure 10: Section-wise Pressure Drop</i>	33
<i>Figure 11: Flow chart for the design of Precooler Heat Exchanger</i>	34
<i>Figure 12: Temperature Profile Validation of counter current HX along the length against saeed et al</i>	35
<i>Figure 13: Counter Flow Temperatures Profile along normalized length</i>	36
<i>Figure 14: Nusselt number and Prandtl Number Profiles of both hot and cold fluid</i>	37
<i>Figure 15: Local thermo-hydraulic factors along the normalized length</i>	38
<i>Figure 16: Heat transfer Uncertainties in Counter flow</i>	39
<i>Figure 17: Relations of local Fanning factor</i>	40
<i>Figure 18: Local Pressure Drop Profile across the normalized length</i>	41
<i>Figure 19: Pressure Distribution across the length for hot and cold fluid</i>	41
<i>Figure 20: Temperature Profile and Dimensionless Temperature Profile</i>	43
<i>Figure 21: Influence of inlet sCO2 Pressure on Pressure Drop characteristics of sCO2</i>	43
<i>Figure 22: Reynolds Number distribution across the normalized length for different sCO2 Pressure</i>	44
<i>Figure 23: Influence of sCO2 inlet pressure Thermohydraulic characteristics of sCO2</i>	44
<i>Figure 24: Effect of water inlet condition on Temperature Profiles across the normalized length</i>	45
<i>Figure 25: Effect of water inlet condition on local Heat Transfer rate</i>	46
<i>Figure 26: Local Pressure Drop characteristics along the normalized length at different water inlet temperatures</i>	47
<i>Figure 27:(a) sCO2 outlet temperature, (b) Total heat transfer rate for the pre-cooler, (c)Total pressure drop characteristics with respect to the water inlet Temperature</i>	48

LIST OF TABLES

<i>Table 1: Thermohydraulic Correlations Review for zigzag channel</i>	<i>17</i>
<i>Table 2: sCO₂ cycle conditions</i>	<i>19</i>
<i>Table 3: Geometric Parameters of Each PCHE Block.....</i>	<i>24</i>
<i>Table 4: Derived Geometric Parameters.....</i>	<i>24</i>
<i>Table 5: PCHE Technical Characteristics</i>	<i>24</i>
<i>Table 6: PCHE network for Full 25 MW class Pre-cooler.....</i>	<i>27</i>
<i>Table 7: Precooler Key Operational parameters and constraints.....</i>	<i>28</i>
<i>Table 8: PCHE Design parameter used in nodal approach.....</i>	<i>32</i>

NOMENCLATURE

A_c	Cross section area of the channel, m ²
A_{ff}	Free flow area, m ²
A_{ht}	Total heat transfer area, m ²
C_p	Specific heat capacity at constant pressure, J/kg·K
d	Channel diameter, mm
D_h	Hydraulic diameter, mm
f	Fanning friction factor
h	Heat transfer coefficient, W/m ² ·K
j	Colburn friction factor
k	Thermal conductivity of the HX material
L_{eff}	Effective Heat transfer length, m
L	Heat transfer length, m
\dot{m}	Mass flow rate, kg/s
N_{ch}	Total number of channels
Nu	Nusselt number
p_l	Longitudinal Channel pitch, mm
p_t	Transverse Channel pitch, mm
P	Perimeter of the channel, m
Pr	Prandtl number
P_{in}	Inlet pressure, MPa
P_{design}	Design pressure, kPa
Q_{th}	Thermal capacity, MW _{th}
Re	Reynolds number

St	Stanton number
t	Plate thickness between channels, mm
t _{eff}	Effective conduction thickness, mm
t _{min}	minimum allowable plate thickness, mm
E	Joint Efficiency, %
T _{in}	Inlet temperature, K
T _{out}	Outlet temperature, K
U	Overall heat transfer coefficient, W/m ² ·K
u	Velocity, m/s
TIT	Turbine Inlet Temperature
sCO ₂	Supercritical CO ₂

SUBSCRIPTS

w	water side of the heat exchanger
H ₂ O	water side of the heat exchanger
s	sCO ₂ side of the heat exchanger
sCO ₂	sCO ₂ side of the heat exchanger
pf	parallel flow
cf	counter flow
xf	cross flow

GREEK

α	Zigzag angle
θ	Fin angle

ρ Density
 σ Maximum allowable stress, MPa
 ΔT_{LM} Log mean temperature difference
 Δp_{fric} Frictional pressure drop, kPa

ABBREVIATIONS

CSP Concentrated solar Power
BC Brayton Cycle
RC Recompression Cycle
ORC Organic Rankine Cycle

CHAPTER ONE

INTRODUCTION

1.1 Background

In this ever-changing global world, there remains crucial environmental issue that affects the climate and imbalance of it in any point leads to the imbalance of the earth. The world has been dependent on fossil fuels from the invention of steam engines. The dependence on fossil fuels for electricity generation has fatalistic impact on the climate due to green-house gas emissions. As an effort to minimize the environmental damage recent trends for sustainable and renewable energy sources has been shown. These new developments are likely to include CSP, Nuclear, and Green Hydrogen Technologies as well as increasing energy efficiency by waste-heat-recovery, and carbon-capture and storage.(Commission, n.d.)(I.R.E.N.A., n.d.). So, the power cycles will possibly remain center of consideration for future energy research.

The sCO₂ recompression cycle can be considered as a potential alternative for the conventional steam Rankine cycles(Katz et al. 2021) in several power generation sectors, such as, CSP at a higher pressure (Luu et al., n.d.)(Yin et al. 2020), nuclear power at high temperature (J H Park et al., n.d.)(Pan Wu et al. 2020)(P Wu et al., n.d.), waste-heat recovery (Marchionni, Bianchi, and Tassou, n.d.)(Bianchi et al., n.d.) (Song et al., n.d.)or even conventional fossil fuel fired powerplants (S. Park et al., n.d.) . Existing power cycles, e.g. the Rankine cycle and the simple Brayton cycle, usually operates with steam and air as working fluid respectively.

Nevertheless, as an effort to achieve higher thermal efficiencies of the power cycle an alternative working fluid is a necessity. The sCO₂ power cycles, per se, is being considered as a promising candidate for having high cycle efficiencies at temperatures ranging from 620K to 1070K. The sCO₂ power cycles also show satisfactory operational pliability to keep up with the rising trend in renewable energy sources (White et al. 2021).

The promise of sCO₂ is underlined by the enormous increase in research over the previous decade, as well as the financial assistance made available globally to promote technical improvement. The thermo-fluid properties of Carbon dioxide e.g. density, viscosity, specific-heat, thermal conductivity show an abrupt fluctuations near pre-

The promise of sCO₂ is underlined by the enormous increase in research over the previous decade, as well as the financial assistance made available globally to promote technical improvement. The thermo-fluid properties of Carbon dioxide e.g. density, viscosity, specific-heat, thermal conductivity show an abrupt fluctuations near pre-cooler operating condition namely the pseudo-critical region(Figure 1). The sCO₂ shows a very high density when cooling near to the critical temperature in the pre-cooler. The compressor requires low power consumption to compress high-density sCO₂ which results in high overall thermal performance of the trans-critical and super-critical CO₂ cycles. As a result, the sCO₂ shows some advantages as the working fluid in the cycle pre-cooler in comparison with supercritical-water as it has a low specific-volume as well as other low critical-parameters.(Ehsan, Guan, and Klimenko 2018).

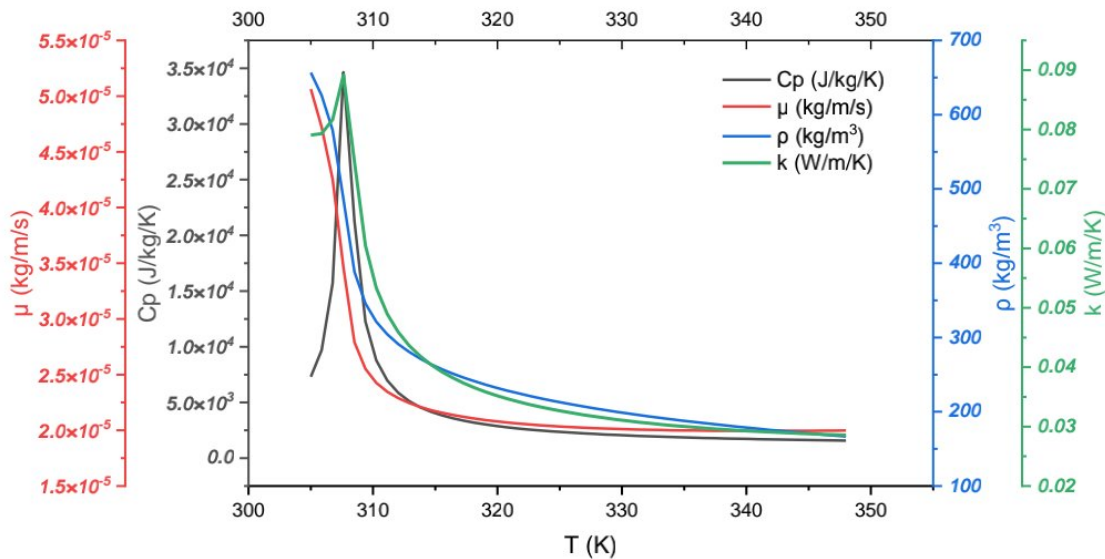


Figure 1: Abrupt change of Carbon dioxide properties(RGP)extracted from CoolProp near the pseudo-critical temperature at Pre-cooler design operating Pressure(8MPa)

1.2 PROBLEM STATEMENT

Printed Circuit Heat Exchangers (Figure 4) are one of the most widely adopted heaters and recuperators for supercritical CO₂ (sCO₂) Recompression Closed Brayton Cycle (RCBC) (White et al. 2021).

Printed Circuit Heat Exchangers (PCHEs) serve as recuperators and pre-coolers in the power cycle, and their design is critical to the cycle's efficiency and design. The recuperators and pre-coolers are significant heat exchange facilities in the system, as well as on the system. security, economy, and stability. The printed circuit heat exchanger is a cutting-edge new technology. Given that PCHEs account for around 80% of the total expenditure in a sCO₂ power cycle (Brun, Friedman, and Dennis 2017), it is essential that their designs be optimized for effective heat transmission and a modest pressure decrease.

Because of their excellent pressure and temperature resistance, compactness, and effectiveness, PCHEs are ideal candidates for the sCO₂ Recompression Brayton cycle, resulting in an 85 percent volume decrease. (Figure 2) versus a shell-and-tube exchangers (Johnston, Levy, and Rumbold 2001).

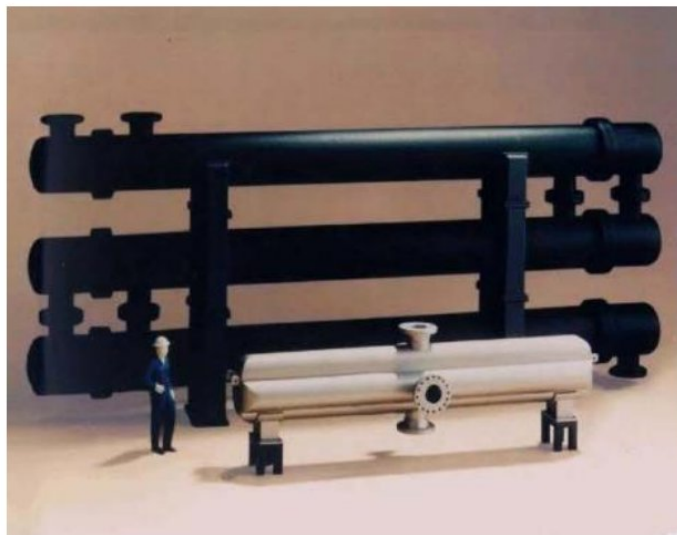


Figure 2: Size comparison of PCHE to STHE

1.3 METHODOLOGY OF THE STUDY

In our study, we proposed the thorough design of a 25MW class Pre-cooler. We validated the the temperature profiles for sCO₂ and water streams with Saeed et al for the same zigzag

channel geometry (Muhammed Saeed, Ali Awais, and Berrouk 2021). We obtained similar temperature profile with that mentioned study. For the in house design code we firstly defined all the geometric parameters for the PCHE channel. Then , we analysed a single module of heat exchanger consisting alternate channel stacks of sCO₂ and water plates. Eventually, we have proposed a combination of PCHE modules for desired heat load.

1.4 ARRANGEMENT

This thesis first introduces the importance of utilizing zigzag channeled PCHE for the pre-cooler of sCO₂ recompression cycle integrated with CSP, was followed by an elaborate literature review. The literature review was done on sCO₂ recompression cycle focusing on CSP application as well as Printed Circuit Heat Exchanger focusing on Zigzag channel and pre-cooler application. In the methodology chapter the physical model mathematical model an iterative nodal approach has been described. The conclusion chapter follows the Results and Discussion chapter for Design and Off- Design condition.

1.5 LIMITATIONS

This study mainly perfomed for single-phase thermo-hydraulic performance of CO₂. No comprehensive comparisons of thermo-hydraulic characteristics for PCHEs with different channel configuration have been carried out. The study will not be applicable for transient state designs.

2 CHAPTER TWO: LITERATURE REVIEW

2.1 REVIEW OF S-CO₂ RECOMPRESSION CYCLE

One of the most promising design variations of the supercritical CO₂-Brayton cycle is the sCO₂ – Recompression cycle. At present, most of the research on recompression cycle is primarily been focused on the supercritical CO₂(Dostal 2004).

The simple BC has higher compactness as the required turbo-machineries are small in size than the ORC with steam as the working fluid. Nevertheless, the BC requires higher compression power to operate that can be eliminated by very high TIT about 1470K or more (H.I.H. Saravanamuttoo, H. Cohen and A.C. Nix 2017). To achieve higher efficiency with low cycle operating temperature steam cannot be used as the working fluid. As a replacement of steam, Helium or Carbon dioxide can be used in a closed cycle configuration. Helium as the working fluid with 1120K – 1220K cycle operating temperature can make the cycle efficiency over 50% while significantly reducing the cycle efficiency at around 770K in BCs for nuclear applications (Herranz, Linares, and Moratilla 2009). This issue can be eliminated using sCO₂ as the working fluid (Pérez-Pichel et al. 2012).

The recent trends of research can be seen on application of sCO₂ cycles integrated with CSP as one of the preventative measures towards the effects of climate change and potential of CSP as a robust non-conventional source of energy. Linares et al. investigated various configurations based on the recompression layout with IC+RH both wet and dry cooling systems (Linares et al. 2020). Recently, Ehsan et al. comprehensively investigated the influence of cooling system design under various working conditions on the optimal performance of sCO₂ recompression cycle as well as an iterative nodal approach for the design and optimization of the air-cooled finned tube HX bundles within the NDDCT (Ehsan, Duniam, Li, et al. 2019). Li et al. surveys the experimental facilities for a comprehensive review on Solar thermal application of sCO₂ power cycles including nuclear, fuel cell and other non-conventional application (M. J. Li et al. 2017). Turchi et al. studied dry cooling for a recompression cycle to reach a cycle efficiency about 50% employed with reheat and inter-cooling, focusing on CSP (Turchi et al. 2013). Milani et al. proposed a recompression with IC+RH integrated with hybrid fossil and solar thermal power plant for low carbon footprints (Milani et al. 2017). Wang et al. proposed a multi-objective optimization approach to determine

the most suitable layout to be recompression with IC and partial cooling in case of high temperature at compressor with dry cooling system (K. Wang et al. 2018).

To employ the recommendation by Dostal printed circuit heat exchangers (PCHE) can be used for sCO₂ power cycles (Dostal 2004). However, Using PCHE as MSHE has some backlashes e.g. clogging, cleaning issue, deterioration of the material due to the molten salt which was observed by several studies (Moore et al. 2010) (Sabharwall et al. 2014) (Lao et al. 2019). In HTR, LTR and Precoolers the aforementioned issues cannot be observed as the operating fluid is sCO₂. Thorough literature review on Precooler application of PCHE will be discussed in the Section 2.2.

2.2 REVIEW ON PCHE

The Printed Circuit Heat Exchanger typically consists of a pair of headers and nozzles acting as inlets and outlets for both hot and cold fluid side as well as a diffusion bonded core containing the flow channels. The diffusion bonding helps to grain structure development across the joint boundaries of parent metal plates resulting a high joint efficiency which exhibits almost same strength and ductility as the parent material. (Brun, Friedman, and Dennis 2017)

These chemically etched micro-channels having a semicircular cross-section significantly enhances the surface area density of the PCHE (Ren et al. 2019).

However, the size of the channel is limited by the thermal performance on the upper limit as for the bigger channel diameter the thermal resistances decreases and smaller channel results large pressure drop for the lower (W. Kim et al. 2017). The depth of semicircular micro channels can typically be 0.5-3mm (Zohuri 2016; Muhammad Saeed et al. 2020).

PCHEs are resilient to extreme operating temperature and pressure of above 1200k and 800MPa while maintaining the effectiveness over 97 (Ji et al. 2009; Le Pierres, Southall, and Osborne 2011).

PCHE can be manufactured using stainless steels and alloys including, stainless e.g. SS304, SS316, SS316L, SS904L, Monel, cupronickel, nickel and super alloys e.g. Inconel 600, Incoloy 800, and Incoloy 825 (Foumeny and Heggs 1991). For this study SS316L has been used.

The PCHEs can have continuous and discontinuous fin configurations (Muhammed Saeed et al. 2020). These two fin configurations can be further decategorized as Straight fins, Zigzag

Fins, S- shaped fins, Airfoil shaped fins, and sinusoidal shaped fin configurations (Cheng et al. 2020; T. H. Kim et al. 2015; Joo Hyun Park et al. 2020; Liu et al. 2020; Nikitin, Kato, and Ishizuka 2007; X. hui Li et al. 2019a; Nikitin, Kato, and Ngo 2006; Ngo et al. 2006; W. Q. Wang et al. 2019; Muhammad Saeed and Kim 2019).

Several cross-sectional shapes have also been developed for continuous fin configurations such as semicircular, rectangular, trapezoidal, triangular (S. G. Kim et al. 2016; Muhammad Saeed and Kim 2017; Ngo et al. 2007; Lee and Kim 2013; Gupta et al. 2008).

Thermo-hydraulic properties of the PCHE of different configurations as discussed above have been determined by both computational and experimental methods. Among all the above-mentioned categories the straight and zigzag channels are mostly used in industrial facilities. The reason for using straight channels is that they are easy and cost effective to manufacture and Zigzag channel PCHE is preferred for its superior thermal-hydraulic characteristics.

Zigzag channel gives significant heat transfer advantages over the straight channel PCHE configuration in laminar flow regions (Chen, Sun, and Christensen 2019). The zigzag channeled PCHEs promotes turbulent flow while preventing the boundary layer formation. They enhance the heat transfer area and the velocity enhancement at bending point elevates the heat transfer performance (Q. Li et al. 2011)

A number of studies on the thermo-hydraulic characteristics has been done using He, sCO₂ and/or water under ranges of Re and Pr to achieve the optimality in heat exchanger(Lee and Kim 2013; Muhammad Saeed and Kim 2017; Chu et al. 2017; Ishizuka et al. 2005; Ngo et al. 2007; Yoon et al. 2017; W. Kim et al. 2017; Huang et al. 2019). But, very few studies has been done on sCO₂ cooling in near critical region.

Baik et al. conducted experimental investigation of zigzag PCHE under cooling condition of sCO₂ in near critical region. They proposed thermo-hydraulic correlations within Prandtl number ranging from 2 to 33 and Reynolds number ranges from 15000 to 100000 for the sCO₂ fluid side. The inlet test conditions on the SCO side was from 7.3 MPa to 8.6 MPa and 26 - 43 °C for pressure and temperature, respectively. Furthermore, they CFD aided investigation and in combination of both methods they developed KAIST_HXD design code. (Baik et al. 2017).

Li et al. investigated the influence of sCO₂ inlet conditions on the thermal performance of Zigzag channeled PCHE. They proposed a new method for estimating the thermal performance

considering the working condition. They showed a relation of overall heat transfer coefficient with operating pressure, temperature, and mass flow rate on supercritical carbon dioxide side suggesting a PCHE will perform better when the working point which is the ratio of average working temperature to pre-cooler temperature, is closer to 1. (X. hui Li et al. 2019b)

Zhang et al. studied computationally considering sCO₂ for both hot and cold side of the zigzag channeled PCHE with zigzag angle ranging from 110° to 130° based on the 1st and 2nd laws of thermodynamics. The inlet condition was considered (390.15 K, 21 MPa) on the Hot side and (295.15 K, 8.5MPa) at the cold side of the PCHE. They discovered the HT enhancement has close relation with the decrement of the generation of entropy as well as the increment of the synergy between temperature and velocity gradient. They demonstrated the result showing that the reverse-flow enhances the field-synergy and reduces the HT entropy-generation whereas the secondary-flow increases the synergy between the temperature as well as velocity gradient in PCHE (Zhang et al. 2019).

Cheng et al. experimentally investigated a 100kW PCHE under test conditions of inlet Re ranging from 31157 to 52806 and inlet temperature varying from 363.4 K to 383.4 K, while the water side inlet Re varied from 1084 to 1947 and the inlet temperature was considered within 293.15 K – 299.7 K. The results suggested an increment of Overall HT performance with increasing Re. On the other hand, the pressure drop on both side of the PCHE decreases with increasing water inlet temperature (Cheng et al. 2020).

Saeed et al. performed a numerical investigation on the thermal-hydraulic characteristics of a zigzag-channeled PCHE with sCO₂ under pre-cooler-conditions. They proposed a new correlation (**Table 1**) for Nu and fanning friction factor for Reynolds number ranging from 5000 to 7000 and valid for Prandtl number of $2.2 < Pr < 13$) on the segmental-averaged values (Muhammad Saeed et al. 2020)

Most Recently, Muhammed Saeed, Ali Awais, and Berrouk's work focused on the CFD based design as well as analysis of a Zigzag-channeled PCHE for the pre-cooler application of a sCO₂-BC under different working conditions (Muhammed Saeed, Ali Awais, and Berrouk 2021).

Table 1: Thermohydraulic Correlations Review for zigzag channel

Literature	Working fluids	Zigzag Angle	Thermohydraulic Correlation	Derivation Type
Nikitin et al. (Nikitin, Kato, and Ngo 2006)	CO2	Hot, $\alpha = 115^\circ$ Cold, $\alpha = 100^\circ$	$f_{p, hot} = (-1.402 \times 10^{-6} \pm 0.087 \times 10^{-6} + (0.04495 \pm 0.00038));$ $2800 \leq Re \leq 5800$ $f_{p, cold} = (-1.545 \times 10^{-6} \pm 0.099 \times 10^{-6} + (0.09318 \pm 0.00090));$ $6200 \leq Re \leq 12100$	Experimental
Ishizuka et al. (Ishizuka et al. 2005)	CO2	$\alpha = 100^\circ$	$h = 0.210Re + 44.16$ $f = -2 \times 10^{-6}Re + 0.1023$ $(5000 \leq Re \leq 13000),$	Experimental
Ngo et al. (Ngo et al. 2007)	CO2	$\alpha = 76^\circ$	$Nu = 0.1696Re^{0.629}Pr^{0.317}$ $; 3.5 \times 10^3 < Re < 2.3 \times 10^4$ $0.75 < Pr < 2.2$ $f = 0.1924Re^{-0.091}$ $; 3.5 \times 10^3 < Re < 2.3 \times 10^4$	Experimental
Baik et al. (Baik et al. 2017)	CO2 - Water	$\alpha = 100^\circ$	$Nu = 0.8405Re^{0.5704}Pr^{1.08};$ $f = 0.0748Re^{-0.19};$ <i>for</i> $15000 < Re < 85000$ $Nu = 0.2829Re^{0.6686};$ $f = 6.9982Re^{-0.766};$ $50 < Re < 200$	Experimental + Computational
Saeed et al. (Muhammad Saeed et al. 2020)	CO2	$\alpha = 100^\circ$	$Nu = 0.475Re^{0.61}Pr^{0.17},$ $f = 0.13Re^{-0.044},$ $(3000 \leq Re \leq 60000)$ $(2.0 \leq Pr \leq 13)$	Computational

3 CHAPTER-THREE: RESEARCH DESIGN

3.1 INTRODUCTION

The design code has been implemented and solved on Python 3.7. The thermo-hydraulic properties of the working fluids has been extracted by coupling the CoolProp (Bell et al. 2014) module with the design code. Similar geometry Zigzag channeled PCHE and correlations was chosen from the experimental study of Baik et al. for the design(Baik et al. 2017). An iterative nodal approach design method which is similar to some of the prior works based on segmental method (Ke et al. 2017)(Guo and Huai 2017) (S. G. Kim et al. 2016)(Bennett and Chen 2019) is implemented.

The inlet Temperature of sCO₂ stream for the Design code is considered to be 348K and the water inlet temperature 292K (Table 7). The cycle design mass flow rate for sCO₂ recompression cycle integrated with CSP is 248.67 kg/s.(Table 2)

The flow stream (10) going towards the main compressor (MC) is wet cooled (Figure 3)by Pre-cooler module

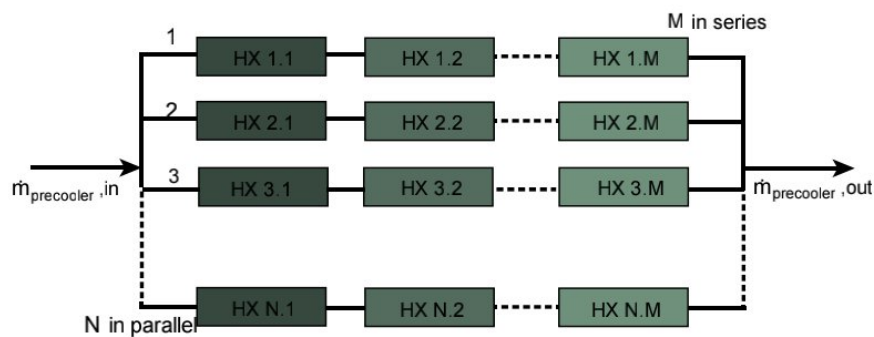


Figure 8) consisting zigzag channel PCHE units.

3.2 sCO₂ RECOMPRESSION CYCLE LAYOUT

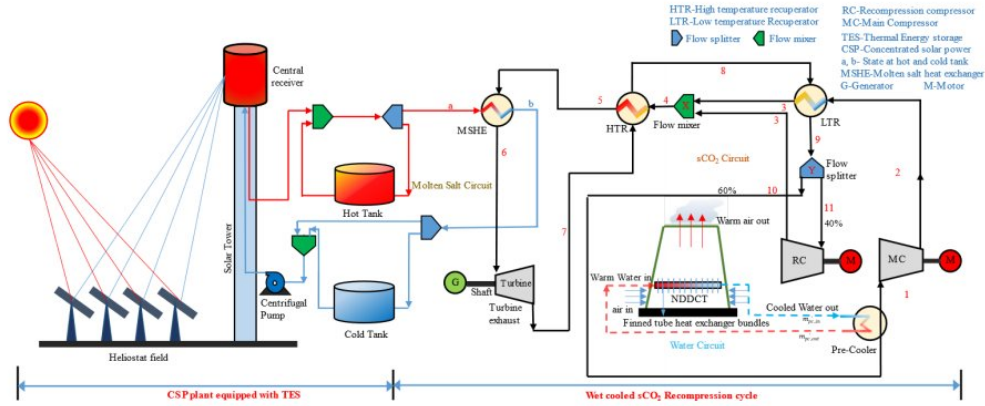


Figure 3: sCO₂ Recompression integrated with CSP

The advantage of recompression cycle (Figure 3) over simple Brayton cycle is that it reduces the pinch point effect occurring inside of a single recuperator.

The effect of pinch point mainly occurs due to the difference of C_p between s . To eliminate this pinch point, ΔT between the lower pressure and higher-pressure stream at several points of the recuperator should be higher than the minimum allowable ΔT which varies for working fluids. However, large temperature gradients reduce the cycle thermal efficiency. The recompression cycle decreases these gradients by reducing the mass flow rates at the higher-pressure side.

This can be achieved by splitting the stream after LTR exit into two streams in a specific ratio (SR). One of the streams follows the recompression cycle path going through the pre-cooler and main compressor. The other goes to the Recompression compressor, where the stream condition is achieved as same as the LTR. The combined flow enters the HTR followed by MSHE where the heat is added to the stream from Solar Tower before entering the Turbine. The Stream going through the MC is cooled by water coming from the NDDCT. (Figure 3)

In addition, split ratio (SR) for a cycle can be defined as the ratio of the mass flow rate of main compressor to the cycle mass flow rate from LTR.

$$SR = \frac{\dot{m}_1}{\dot{m}_9} = \frac{\dot{m}_{10}}{\dot{m}_{10} + \dot{m}_{11}}$$

For this study the split ratio is considered to be 0.6, giving the main compressor i.e. pre-cooler mass flow rate 149.2 kg/s.(**Table 2**)

Table 2: sCO₂ cycle conditions

Parameters	Values
Cycle mass flow rate	248.67 kg/s
Main compressor mass flow rate	149.20 kg/s
SR	0.6

3.3 PHYSICAL MODEL

A module of 26MW diffusion bonded zigzag channeled PCHE is considered for design.

The joint efficiency of typical joint is considered to be 0.7 (Y. W. Kim, Kang, and Kim 2018). The material considered for this design is SST316 that can endure 20000psi stress and shows high thermal-conductivity and resistance to corrosion even in extreme temperatures ranging from 240K to 1270K according to “Section II Part D ASME Boiler and Pressure Vessel Code” (The American Society of Mechanical Engineers (ASME) 2010).

After selecting the flow pattern and cross-sectional form of the channels of heat exchanger, the thickness of the plate solid wall in between the neighboring channel must be addressed for the design of compact heat exchangers. In accordance with the heat exchanger design part of “ASME Boiler and Pressure Vessel Code” (The American Society of Mechanical Engineers (ASME) 2011), the required minimum plate thickness can be calculated by the following formula for semi-circular channels is,

$$t_{min} = PR / (SE - 0.6P)$$

where P is internal-design pressure, R is the channel-radius, S is the max allowable normal stress for the material used and Joint efficiency E .

The maximum allowable design pressure inside a standard printed circuit heat exchanger may be upto 500bars of gauge pressure.

The split view of PCHE single unit with diffusion bonded core was shown in Figure 4.

Table 3 summarizes all the Geometric parameters which are pre-defined. The channel configuration and geometries of PCHE for pre-cooler prototype designed is shown in Figure 6.

A 1.8 mm thick SS316L stainless steel plate is considered to contain 32 chemically-etched channels. The minimum allowable wall thickness is 1.517 mm according to ASME as previously mentioned. For this study the minimum wall thick is 1.52mm which fulfills the requirement. 56 such plates are stacked in Alternate channel configuration giving the total number of channels to be 896

The Figure 7 shows the characteristics lengths of hot and cold side of the heat exchanger.

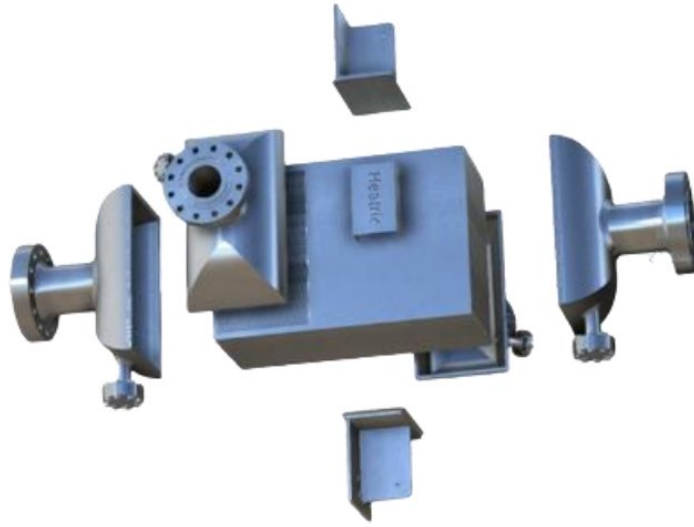


Figure 4: Split view of PCHE (Courtesy MEGGIT("Printed Circuit Heat Exchangers - Meggitt" n.d.))

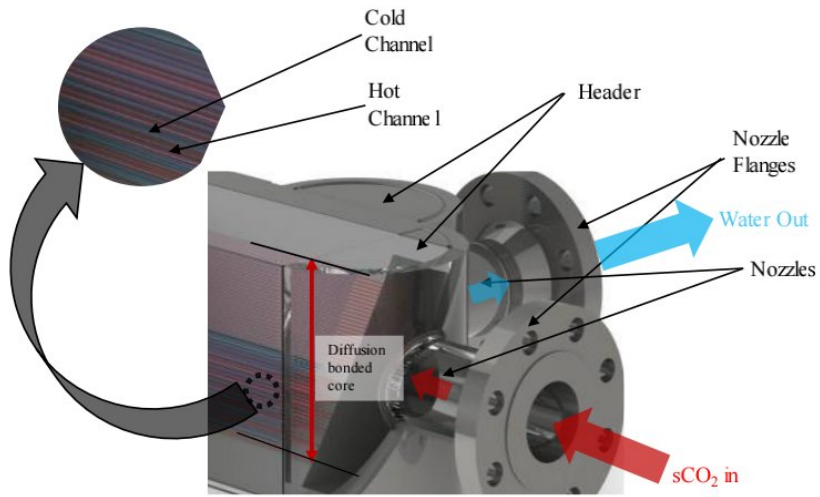


Figure 5: The 3D view for channel configuration and nozzle flanges

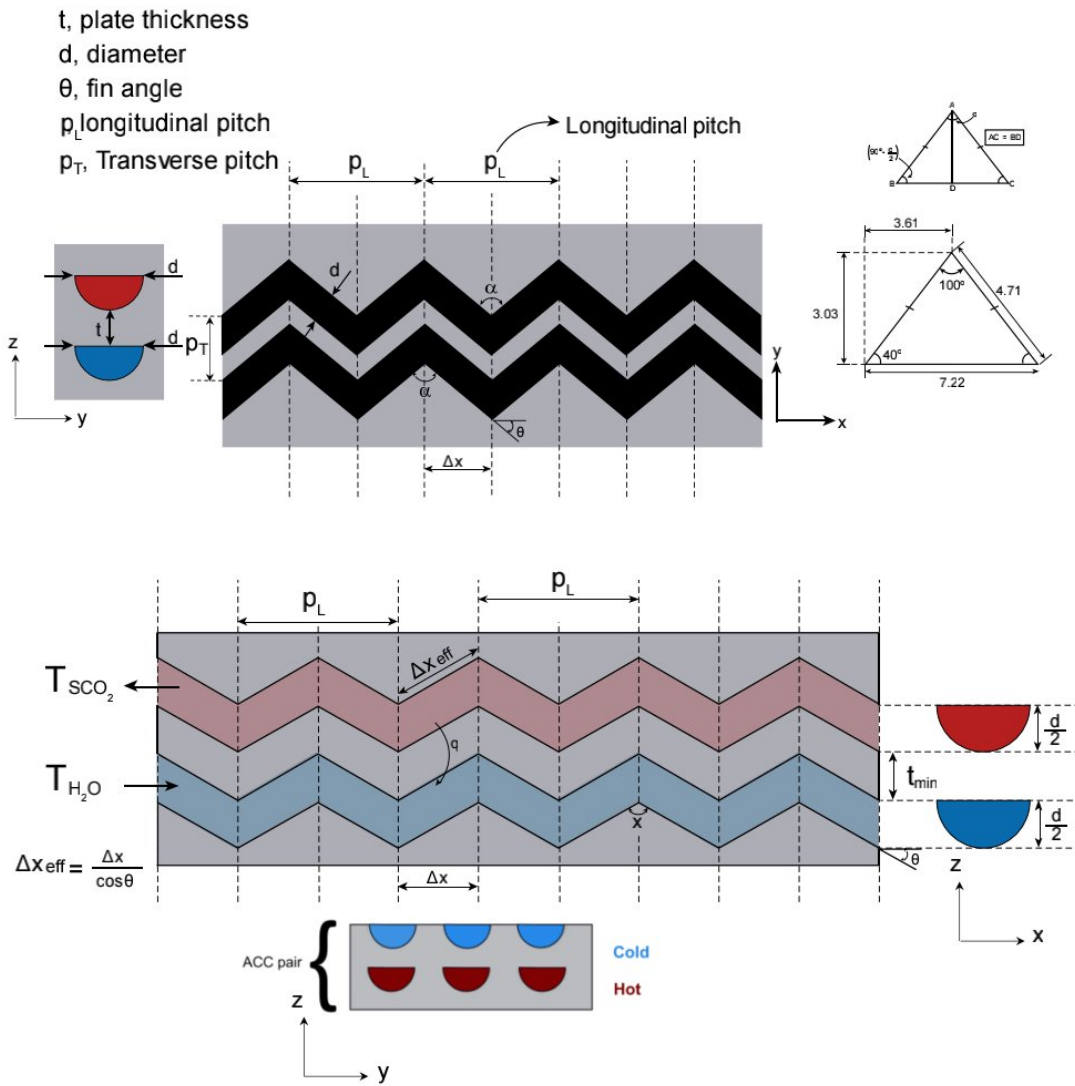


Figure 6: Zigzag Channel Geometry

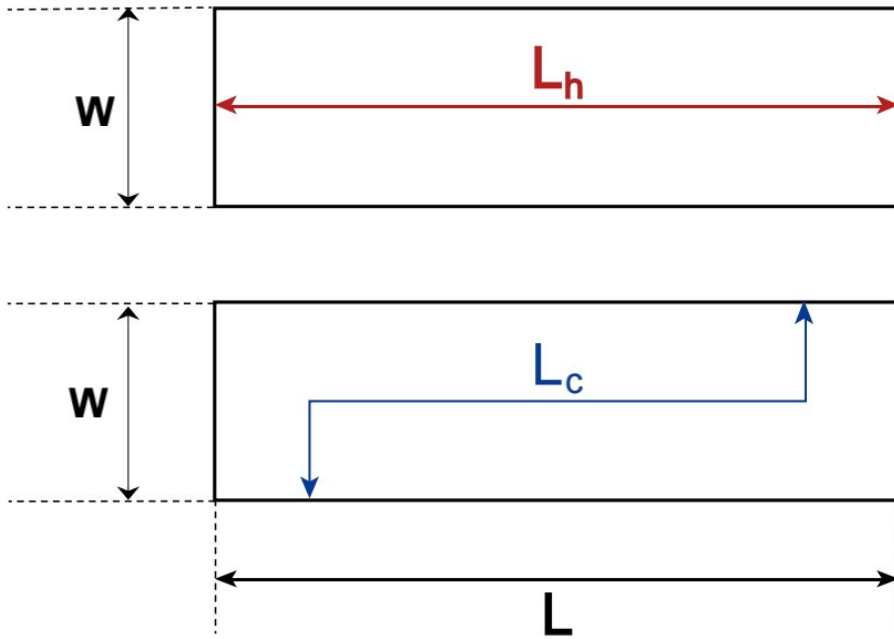


Figure 7: Characteristics Length of Hot and Cold Channels

Table 3: Geometric Parameters of Each PCHE Block

Parameter	Value	Unit
Length	1.5	m
Height	0.5	m
Width	0.5	m
Channel Diameter	1.8	mm
Channel Zigzag angle, alpha	100	degree
Fin angle, theta	40	degree
Fin thickness	3.0	mm
Transverse Pitch (y-axis)	2.35	mm
Longitudinal Pitch (x-axis)	7.22	mm
Pitch along Height (z-axis)	2.55	mm

Table 4: Derived Geometric Parameters

Parameter	Value	Unit
Available Free flow area on each side	9120.19	mm ²
Assumed Effective Plate Thickness	3.05	mm
Total Heat Transfer Area	1802.7821137384228	m ²

Table 5: PCHE Technical Characteristics

Parameter	Value	Unit
Plate Material	Alloy-SST-316	-
Thermal Conductivity	16.4	W/m/k
Maximum Allowable Stress	20000	psi
Diffusion bond joint Efficiency	0.7	-
Internal Design Pressure	500	barg
Minimum allowable Plate thickness	1.517451	mm

3.3.1 EQUATIONS FOR DEFINING CHANNEL GEOMETRY

The cross-sectional area, A_c , and perimeter, P , of a semicircular channel can be calculated from the relations;

$$A_c = \frac{\pi d^2}{8}$$
$$P = \frac{\pi d}{2} + d$$

Hydraulic Diameter,

$$D_h = \frac{4 \times \text{free-flow area}}{\text{wetted perimeter}} = \frac{4 \left(\frac{\pi d^2}{8} \right)}{\frac{\pi d}{2} + d}$$

Available free flow area for the sCO₂,

$$A_{ff} = A_c \times N_{ch}$$

Total free flow area of the heat exchanger,

$$A_{ff} = A_c \times N_{ch}$$
$$L_{eff} = \frac{L}{\cos \left(90^\circ - \frac{\alpha}{2} \right)} = \frac{L}{\cos \theta}$$

The heat transfer area,

$$A_{ht} = L_{eff} \times P \times N_{ch}$$

Inner Cross-sectional area for each water,

$$A_c = \frac{\pi d^2}{8}$$

Available total free flow area for fluid flow,

$$A_{ff} = A_c \times N_{ch}$$

Let W , H , and L be the width, height and length of the heat exchanger respectively. The number of channels along width and height, given by N_w and N_H respectively, are defined as,

$$N_w = \frac{W}{p_T}$$

$$N_H = \frac{H}{p_Z}$$

where, $2 N_{ch} = N_w N_H$

The the effective physical-conduction thickness will vary along the semicircular locus between neighboring channels, i.e. $t_{plate} \leq x \leq p_Z$ so the effective thickness can be defined as the mean of the upper limit and lower limit,

$$t_{eff} = \bar{t} = \frac{p_Z + t_{plate}}{2}$$

The effective thickness for the plate is taken into account for merely the thermodynamic consideration as a compensation for the shape factor while determining the wall thermal resistance.

3.3.2 PCHE COMBINATION

The designed PCHE modules need to be combined in series and/or parallel network to get required heat rejection at a pre-determined mass flow rate.

However, The number of PCHE single units in the series or parallel combination is limited by the pinch point effect. In the series combination the length of the HX units increases by the factor of M (

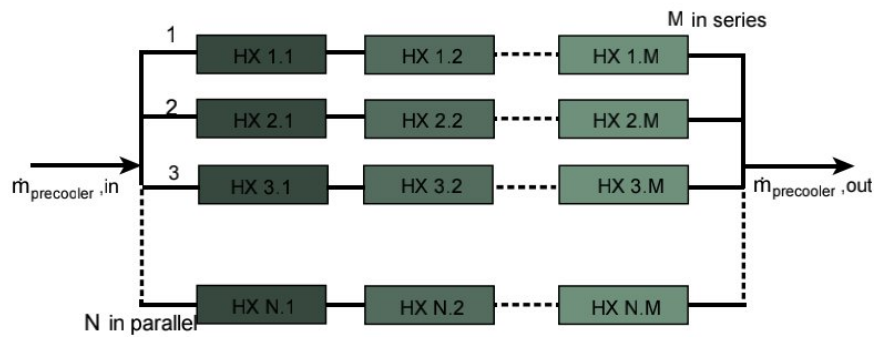


Figure 8). The pre-cooler mass flow splits into N number of streams for the parallel combination. The capacity of the Heat Exchanger will be multiplied by the total number of PCHE single units ($N \cdot M$).

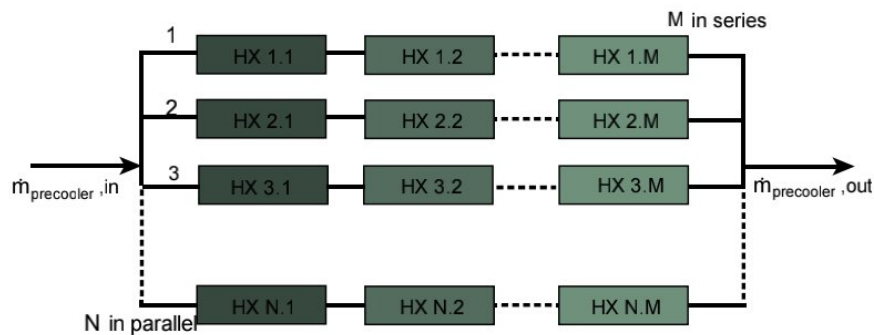


Figure 8 depicts the PCHE network for pre-cooler. Nonetheless, the Heat rejection for each unit may not be the same as the Temperature difference decreases along the length. Eventually, pinch point effect will occur.

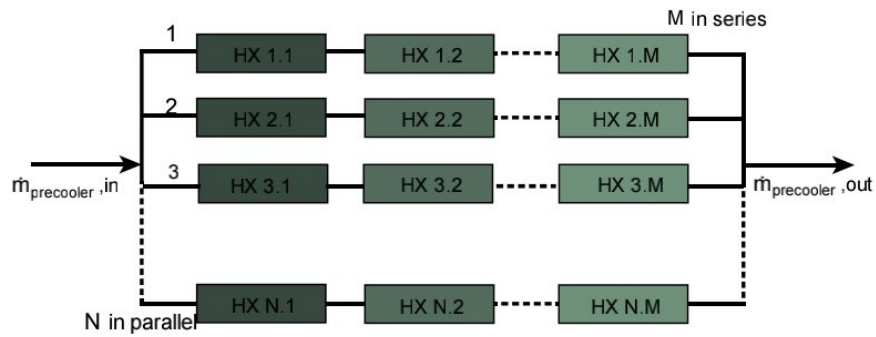


Figure 8: PCHE module combination for required Heat Rejection

For this study, the optimum number of rows of the Pre-cooler unit is 334, giving the mass flow rate for each channel 0.5 g/s. Such two stacks need to be put in series to get the required capacity of the Pre-cooler without encountering any pinch point. (Table 6)

Table 6: PCHE network for Full 25 MW class Pre-cooler

PCHE units in Series, M	2
PCHE units in Parallel, N	334
Number of total units, N*M	2*334

3.4 MATHEMATICAL MODEL

3.4.1 ASSUMPTIONS

The heat exchanger would operate under steady-state condition, i.e., operate with constant flow rates and fluid temperatures (both at the inlet and within the heat exchanger) independent of time. Heat losses to and from the surroundings are neglected.

Non-existence of thermal energy sources or sinks in the heat exchanger. The wall thermal resistance is assumed as a constant and uniform in the entire heat exchanger. No phase change, since we are only dealing with CO₂ gas on one side and water on the other side of the exchanger.

3.4.2 BOUNDARY CONDITIONS

The boundary condition for the design code is elaborately mentioned in Table 7. The hot channel and cold channel are in counter flow configuration as a result the pinch point mentioned is the local temperature difference at a particular node. Cold side mass flow rate has been considered based on initial energy balance.(Figure 11)

Table 7: Precooler Key Operational parameters and constraints

Parameter	Design Values	Off-Design Constraints	Unit
Heat Exchanger load Capacity , Q_{hx} (MWth)	23.85	24 - 27	MW
Cold side inlet temperature, $T_{IN,H2O}$	20	15-25	(°C)
Hot side temperature, $T_{IN,CO2}$ (°C)	75	65 - 105	(°C)
Hot side outlet temperature, $T_{OUT,CO2}$ (°C)	33.13	33-39	(°C)
Cold(water) side inlet pressure, P_{IN} (MPa)	0.101325*1.2	±2%	MPa
Hot(sCO ₂) side inlet pressure, $P_{IN,SCO2}$ (MPa)	8MPa	7 - 10	MPa
Cold mass flow rate (kg/s), M_w	522.27	298.44-596.88	kg/s
Cycle mass flow rate(kg/s), M_s	149.2	-	kg/s
Pressure drop constraints (hot and cold)	<2% P_{IN}	-	-
Pinch point temperature	>5	>5	K

3.4.3 Nodal approach

A single unit PCHE of pre-cooler prototype is divided into $N_x = 38$ sections (**Error! Reference source not found.**) along the length to capture the abrupt fluctuations of sCO₂ at near-critical region. As a result the effective length of each section becomes 7.728 mm while the sectional characteristics length is 5.92mm (Table 8). To, initialize the calculation, for the 38th section meaning the 39th node the inlet temperature of sCO₂ is known and water outlet temperature is assumed. After solving the nth section using steady state energy balance, the outlet condition for a particular section is considered to be the inlet of the section before it for the sCO₂ stream and the inlet of that section will be the outlet for water stream as the hot and cold streams are in counter flow configuration.(Figure 9)

The local steady state energy balance equation is considered to be,

$$\dot{Q}_{hx,local}^j = \dot{m}_s(h_{s,local}^{j-1} - h_{s,local}^j) = \dot{m}_w (h_{s,local}^j - h_{s,local}^{j-1})$$

Where , h represents the enthalpy of the fluids.

The heat transfer correlations used in this design code experimentally derived by Baik et for $2000 < Re < 58,000$ on the hot side sCO₂ as the working fluid(Baik et al. 2017).

For the cold side the flow considered strictly laminar.

Baik et al. suggested the following correlations for the sCO₂ heat transfer coefficient,

$$Nu_s = 0.0293(Re_s)^{0.8138}$$

For lower Reynolds number ($30 \leq Re \leq 400$) on the water side as this one the preferred correlation is Baik et al. (Baik et al. 2017),

$$h_w = 11.04 Re_w + 570.36$$

To evaluate the Reynolds number on both side the the following equation has been used for the both side .of the PCHE.

$$Re = \frac{D_h G}{\mu}$$

Here, G is the mass flux for available free flow area (A_{ff}) for corresponding streams.

The overall HT coefficient can calculated from the following Equation,

$$R_{overall} = R_{sCO2} + R_{plate} + R_{water}$$

$$\frac{1}{U_o} = \frac{1}{h_s} + \frac{t_{eff}}{k_{plate}} + \frac{1}{h_w}$$

Where, k represents the plate thermal conductivity(16.2 W/m K)Heat Transfer area is same for hot and cold side ($A_{ht} = A_{sCO2} = A_{H2O}$). Heat transfer co-efficient for the sCO2 flow stream is defined as,

$$h_s = \frac{Nu_s k_s}{D_h}$$

However, for finding the sectional values of overall HT coefficient,

$$\frac{1}{U_{o,local}^j} = \frac{1}{h_s(T_{s,local}^j, P_{s,local}^j)} + \frac{t_{eff}}{k_{plate}} + \frac{1}{h_w(T_{w,in})}$$

The local values of LMTD is taken as function inlet and outlet temperature of a particular section for counter current flow.

$$\Delta T_{lm,cf}(Ts_{inlocal}, Tw_{inlocal}, Ts_{outlocal}, Tw_{outlocal}) = \Delta T_{lm,local}^j$$

$$\Delta T_{lm,cf} = \frac{(T_{h,in} - T_{c,out}) - (T_{h,out} - T_{c,in})}{\ln \left(\frac{T_{h,in} - T_{c,out}}{T_{h,out} - T_{c,in}} \right)}$$

The correction factor for counter flow is assumed to be 1 i.e. $F_{cf} = 1$. However, near the header region the hot and cold channel is needed to be in cross-flow region. The LMTD correction factor for cross-flow cannot as same as that of counter flow i.e. $0 < F_{xf} < 1$. The correction factor for cross-flow s considered to be, $F_{xf} = 0.987$ (W. Kim et al. 2017). The cross flow LMTD becomes,

$$\Delta T_{lm,xf} = F_{xf} \Delta T_{lm,cf}$$

\bar{F} is the length wise averaged correction factor considered for design code simplification.

$$\frac{\sum_0^{0.15L} F_{xf} + \sum_{0.15L}^{0.85L} F_{cf} + \sum_{0.85L}^L F_{xf}}{L} = \bar{F}$$

The 1st bend in the channel starts at 15% of the effective length of the heat exchanger which results the cross flow between the water and sCO2 channels followed by counter flow region. At the end, from 15% from the 2nd header is considered to be in cross flow configuration.

So, the Heat Transfer capacity for a single section PCHE is defined as,

$$\dot{Q}_{hx,local}^j = U_{o,local}^j \delta A_{ht} \bar{F} \Delta T_{lm,local}^j$$

$$\frac{A_{ht}}{Nx} = \delta A_{ht}$$

The definition for the Colburn j factor (Shah and Sekuli 2003) for respective hot and cold side is,

$$j_c = St \cdot Pr^{2/3} = (Nu \cdot Pr^{-1/3})/Re$$

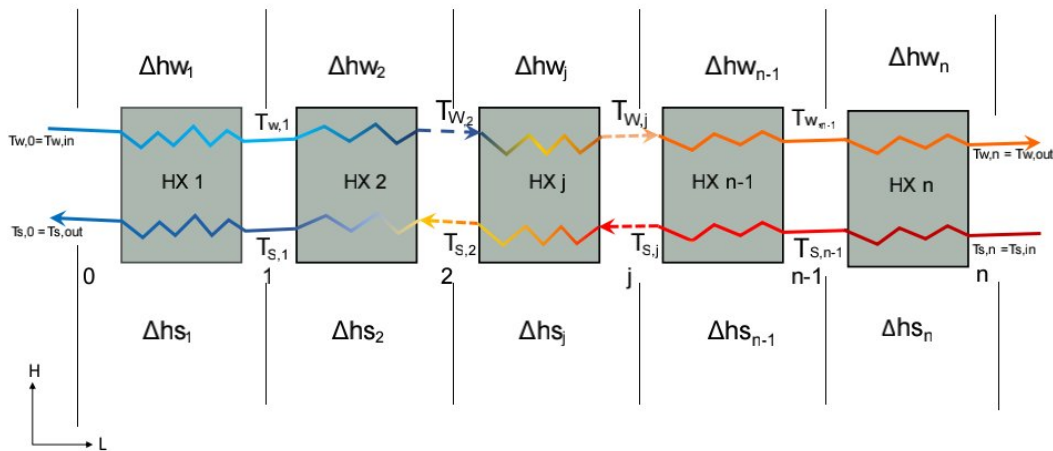


Figure 9: Nodal Approach across the length.

Table 8: PCHE Design parameter used in nodal approach

Parameter	Value	Unit
Number of channels on each side, Nch	896	-
Length of Concern	225	mm
Effective Length	293.7166	m
Counter flow Length	0.70* L _{eff}	m
Cross flow Length	0.15* L _{eff}	m
Number of Nodes, n+1	39	-
Number of Sections, n	38	-
Sectional Length	5.92	mm
Sectional Heat Transfer Area, δA _{ht}	47.849327858796265	m ²

3.4.3.1 Uncertainties consideration in Heat Transfer

The sectional uncertainty for the heat transfer rate is considered with respect to the sectional heat rejection by sCO₂ stream to get the better evaluation of heat transfer rate as an effort to compensate the property fluctuation of sCO₂, and can be calculate by the following equations.

$$Error_{hx,local}^j = \frac{|\dot{Q}_{hx,local}^{j+1} - Q_{sCO_2}^j|}{Q_{sCO_2}^j}$$

$$\sum_{i=0}^{i=n-1} \dot{Q}_{HX,sectional} \pm \sum_{i=0}^{i=n-1} Error_{HX,sectional} = Q_{HX}$$

$$\dot{Q}_{HX} = \dot{Q}_{sCO_2} = \dot{Q}_{H_2O}$$

3.4.3.2 Pressure Drop

The pressure is considered within the channels while neglecting the pressure drop through the header region. The nodal approach is applied to evaluate the pressure drop on both hot and cold side of a single PCHE. Figure 10 depicts nodal approach for determining the local pressure drop on the sCO₂ side.

To capture the abrupt fluctuations in properties of the sCO₂ local density and local fanning friction factor has been considered.

$$\Delta P_{s,local} = \Delta P_s(\rho_s(T_{s,local}, P_{s,local}), f_s(T_{s,local}, P_{s,local}))$$

Where, The friction factor used in this study was derived experimentally by Baik et al. (Baik et al. 2017)

$$f_s = 0.2515 Re^{-0.2031}$$

And the frictional pressure drop can be determined from the following equation,

$$\Delta P_s = \frac{2f_s G_s^2 L_{eff}}{D_h \rho_s}$$

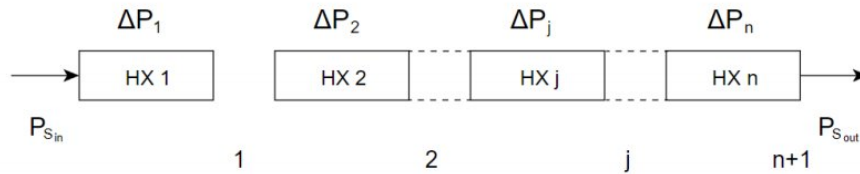


Figure 10: Section-wise Pressure Drop

For the water side of the heat exchanger the properties of the water is considered merely in the bulk mean temperature as the low temperature and the pressure change on the water side does not have the any significant influence on the properties of water.

$$\Delta P_{w,local} = \Delta P_s(\rho_s(T_{w,local}), f_s(T_{w,local}))$$

Where, the fanning friction factor (Baik et al. 2017) is defined as,

$$f_w = 1.3856 Re^{-0.482}$$

The pressure drop on the water side,

$$\Delta P_w = \frac{2f_w G_w^2 L_{eff}}{D_h \rho_w}$$

The dimensionless Euler number (Shah and Sekuli 2003) for both hot and cold of the PCHE can be determined from,

$$Eu = \Delta P^* = \frac{\Delta P}{\rho u_{m^2}/2G}$$

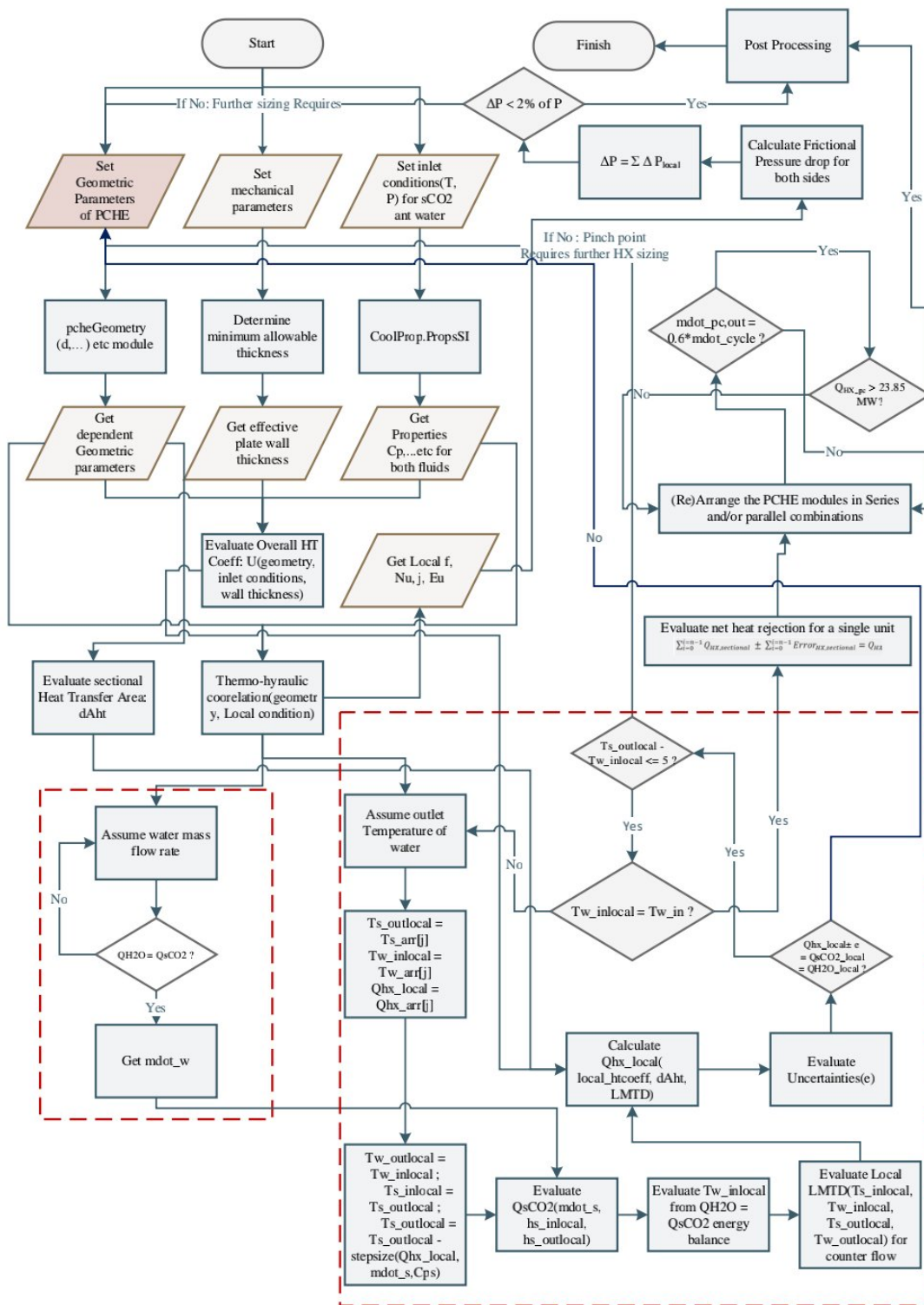


Figure 11: Flow chart for the design of Precooler Heat Exchanger

3.5 CODE VALIDATION

The design code is validated against Muhammad Saeed's CFD aided design (Muhammed Saeed, Ali Awais, and Berrouk 2021). The similar geometry of each channel is considered to be Zigzag configuration with semicircular with fin angle of 40°. The design code of Muhammad Saeed et al. consisting of 144 segments along the length to allow Prandtl number range of 1 – 13.

The temperature profile from Muhammad Saeed's study with sCO₂ inlet Temperature of 70°C and mass flow rate of each channel 0.5g/s is considered for the validation.

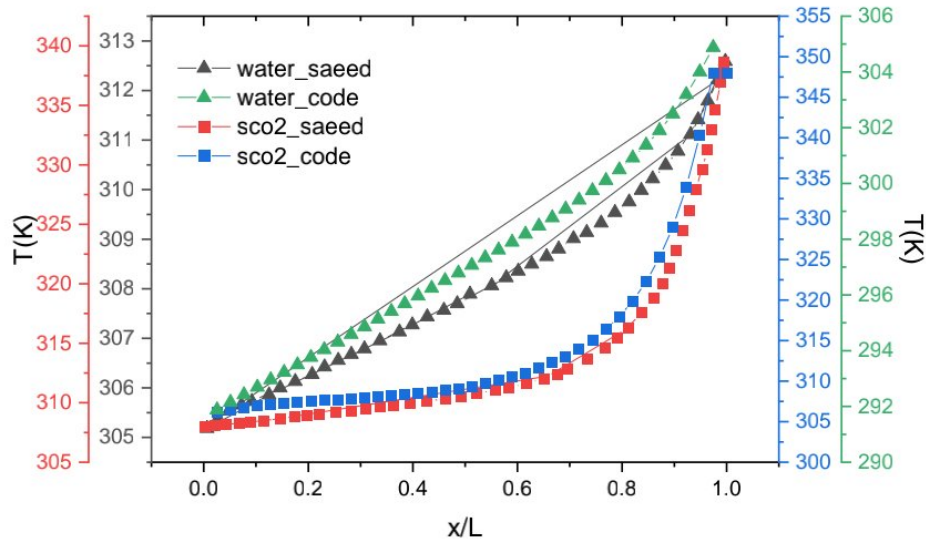


Figure 12: Temperature Profile Validation of counter current HX along the length against saeed et al

4 CHAPTER-FOUR: DATA GENERATION / COLLECTION, ANALYSIS AND DISCUSSION

4.1 TEMPERATURE PROFILES

Figure 13 demonstrates distribution of the temperature profile of sCO₂ and the water coolant along the normalized length of the pre-cooler. The temperature profile for sCO₂ is steeper than that of water as sCO₂ possesses superior heat transfer properties than water. The inlet temperature of sCO₂ is 348 K operating under a pressure of 8MPa. The water inlet temperature is esteemed to be 291.87 K with 1.2 MPa. However, the inlet water pressure is supposed to be atmospheric pressure but the pressure-drop induced to the fluid may have potential to create a vacuum followed by a backpressure at outlet of the cold side. So, in order to compensate that back pressure, the water should be pumped a slightly higher pressure than mere the atmospheric pressure.

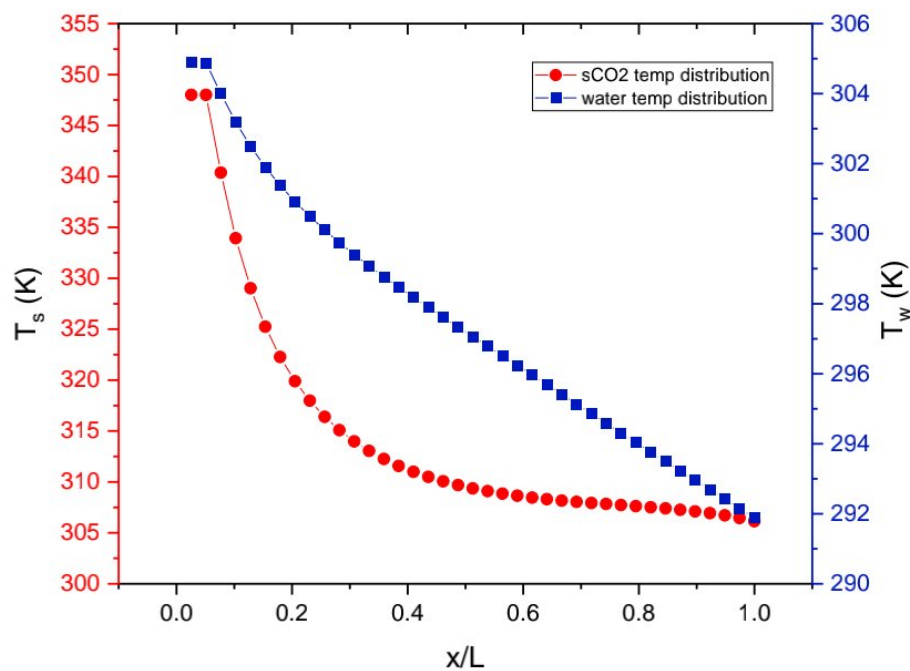


Figure 13: Counter Flow Temperatures Profile along normalized length

4.2 HEAT TRANSFER CHARACTERISTICS

Figure 14 illustrates the Nusselt number and Prandtl number distribution as a manifestation of thermodynamic performance of the Pre-cooler. The Nusselt number of sCO₂ ranging from 104.5 to 54.6 for the cooling operation clarifies the Heat Exchangers designed for HTR and LTR is not applicable for pre-cooler operation.

The design code has been developed under Prandtl number of 1 to 13. The maximum Prandtl number reaches at the Pseudo-critical point of sCO₂. However, the Prandtl number of water varies only from 5 to 7.

The dimensionless heat transfer co-efficient, the Colburn j factor shows almost a linear trend. Nonetheless, the Colburn factor is significantly higher for each section of the pre-cooler for sCO₂ than that of water as sCO₂ has higher heat transfer properties than water, shown in Figure 15

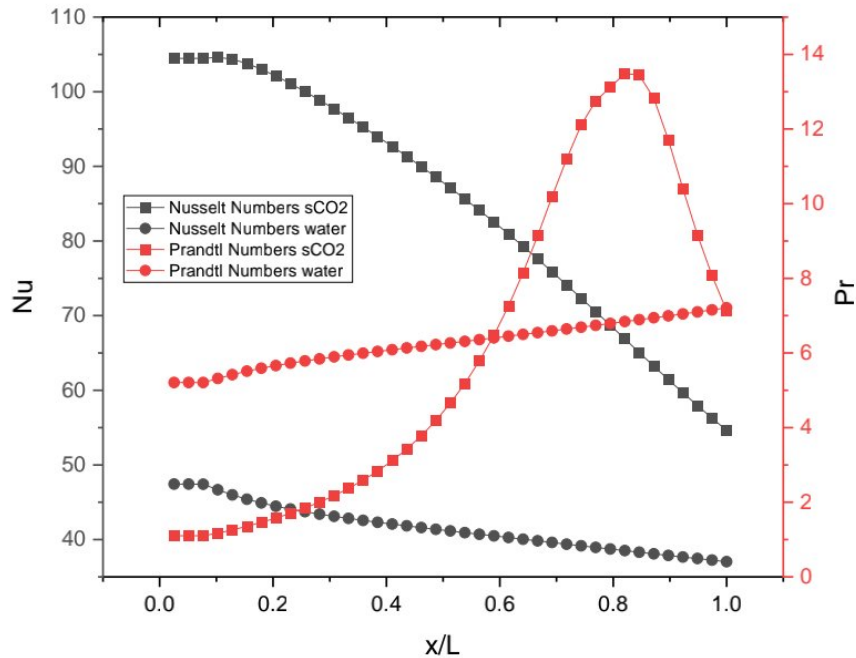


Figure 14: Nusselt number and Prandtl Number Profiles of both hot and cold fluid

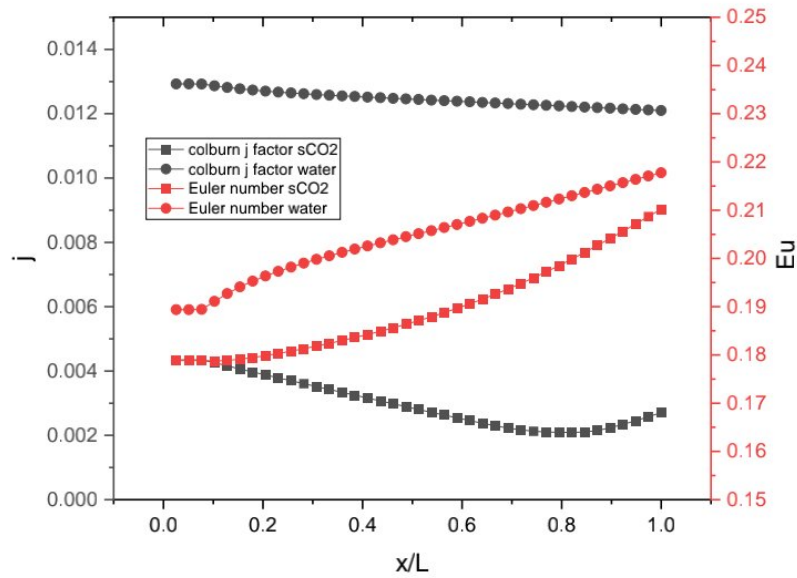


Figure 15: Local thermo-hydraulic factors along the normalized length

4.2.1 Uncertainties

Figure 16 exemplifies the uncertainties associated with local heat transfer rate due to the abrupt fluctuations of sCO₂ properties. The local heat transfer rate would be higher at the beginning as the local temperature difference is high. Then the heat transfer rate shows gradual decline as the temperature difference reduces. However, the heat transfer rate shows a slight increment as the thermodynamic properties enhances near the critical point. The sectional uncertainties rise up when the sCO₂ reaches about 20% of the length followed by a gradual decline as the sCO₂ approaches the pseudo-critical region. The error becomes only 0.2% when the sCO₂ temperature reaches 307.83 K which is near to the pseudo-critical region.

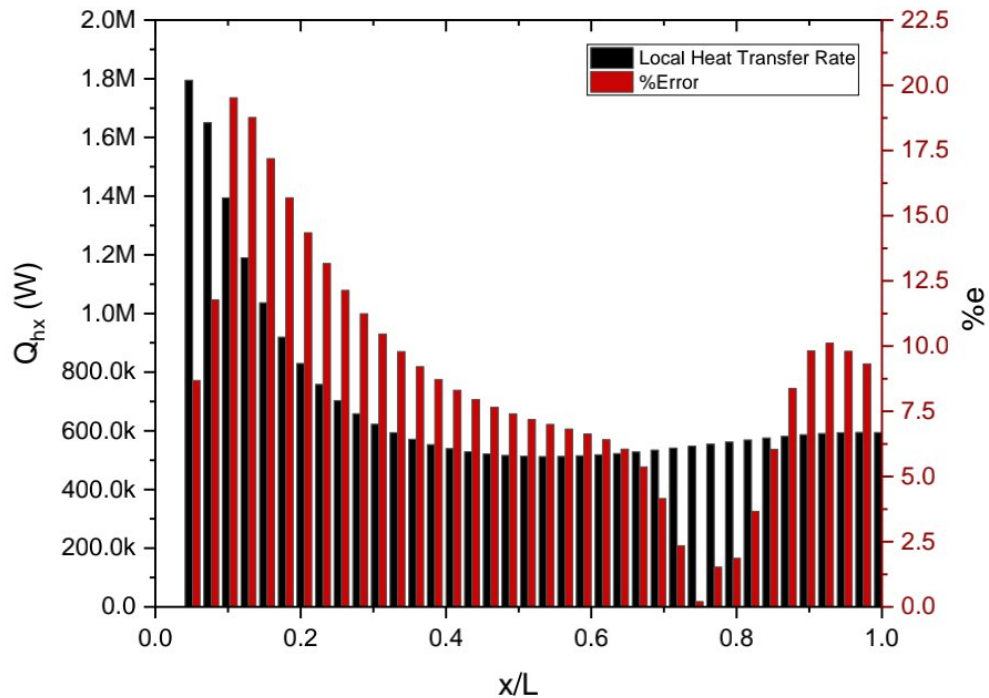


Figure 16: Heat transfer Uncertainties in Counter flow

4.3 PRESSURE DROP CHARACTERISTICS

Figure 17 demonstrates the Fanning friction factor as function of normalized length and relation with Reynolds number. The local Fanning factor of sCO₂ shows a steady inclination. However, the friction factor for each section on the water side is surprisingly higher than that of sCO₂

The Reynolds number of water remains fairly similar across the normalized length of the pre-cooler whereas the Reynolds number for sCO₂ gradually decreases. The changes in the trend of Reynolds number significantly affects the Pressure drop characteristics, which will be discussed later in this section 4.3.

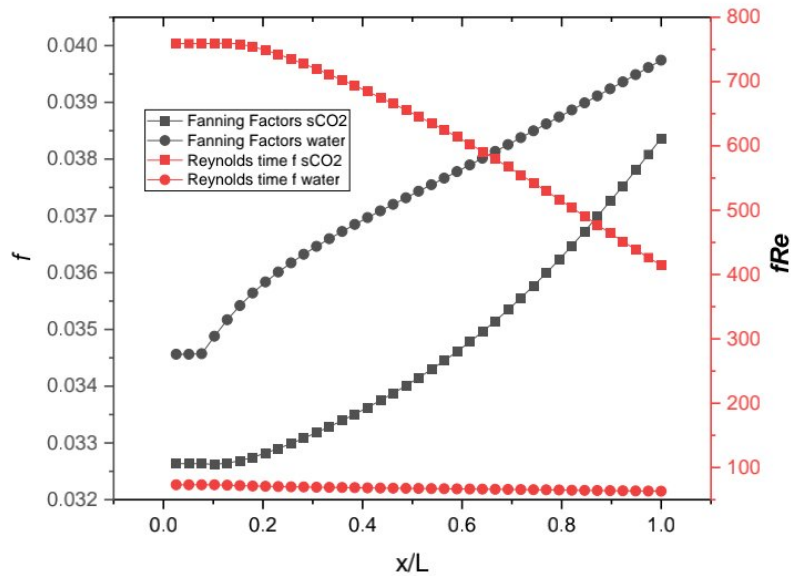


Figure 17: Relations of local Fanning factor

The sectional pressure drop variations of each fluid across the normalized length has been illustrated in Figure 18.

The inlet for the sCO₂ is the 0% of the normalized length meaning at the first node and for water it is 100% of the normalized length which means at the last node.

The local pressure drop for sCO₂ is dominating at the inlet section of the pre-cooler because of the high Reynolds number and gradually declines. Nevertheless, the pressure drop on the water side is more than that of sCO₂ side. Because, near the pseudo-critical region the density of sCO₂ becomes high so the pressure drop reduces along the length and the Reynolds number across the length of the water remains fairly constant, as depicted in Figure 17. Consequently, the sCO₂ pressure distribution shows a convex trend whereas the water pressure distribution shows a concave trend, as shown in Figure 19.

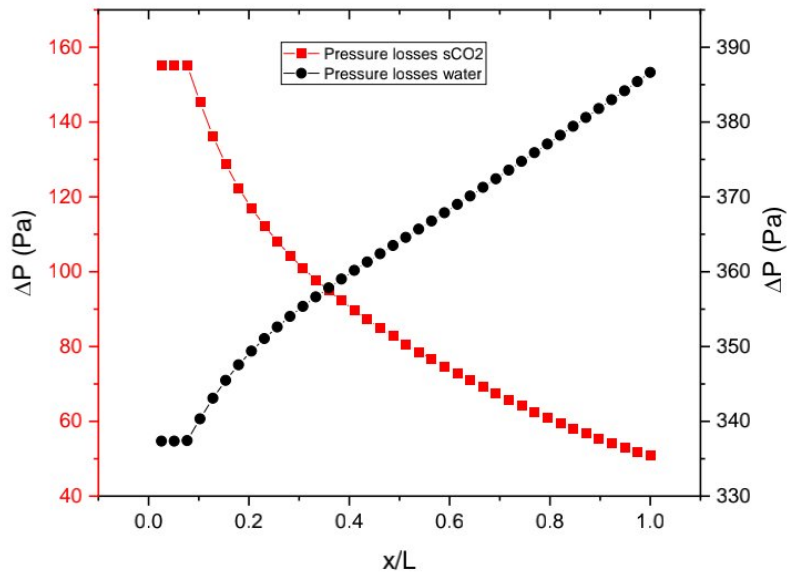


Figure 18: Local Pressure Drop Profile across the normalized length

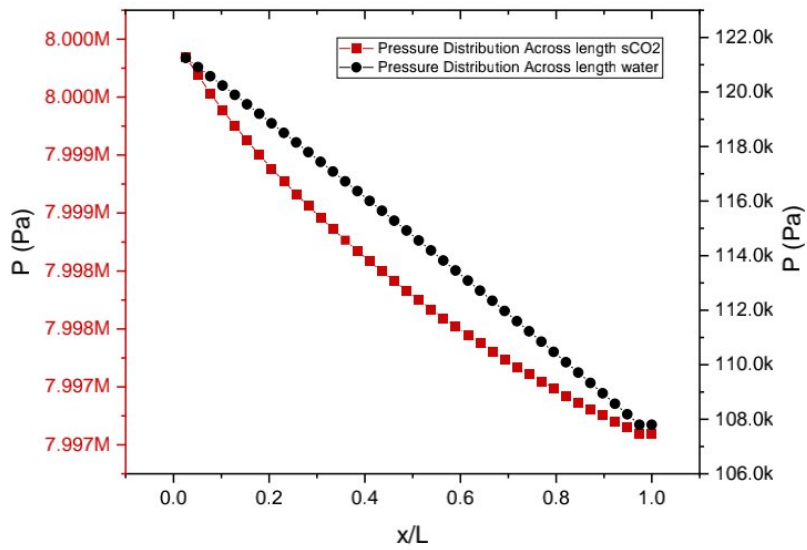


Figure 19: Pressure Distribution across the length for hot and cold fluid

4.4 OFF DESIGN

For the analysis of the Off-design performance of the heat exchanger the effect on the change of the following parameters are considered while keeping the other parameters in design condition.

4.4.1 Effect of sCO₂ Inlet Pressure

The Off-design thermo-hydraulic performance for the sCO₂ inlet pressures of 7MPa, 7.5MPa, 8.5MPa, 9 MPa ,10MPa has been investigated.

The effect of the operating pressures of sCO₂ has been Temperature profile and Nusselt number is illustrated in Figure 20. The increasing sCO₂ operating pressure increases the outlet temperature of sCO₂. The theoretical outlet temperature of sCO₂ is 302K under 7MPa operating pressure whereas 308.59K for operating pressure 8.5MPa. However, at 9MPa and 10MPa outlet Temperatures shows a slight reduction of 1.2K and 2K respectively. The range of local Nusselt numbers significantly reduces with the increase of sCO₂ inlet pressure.

The effect of variation of sCO₂ inlet pressure on the pressure drop characteristics is demonstrated in Figure 21. The increment of the operating pressure of the working fluid depreciates the net pressure drop across the length of the pre-cooler as the thermo-hydraulic characteristics become staunch at the far-critical regions. Nonetheless, the Euler number increases with the increase of operation pressure.

Figure 22 manifests the local Reynolds Number distribution across the normalized length with the variation of sCO₂ inlet pressure. The Reynolds number shows notable reduction with increasing operating pressure.

The influence of sCO₂ inlet pressure on Fanning Factor and Colburn factor with Reynolds number is exemplified in Figure 23. The Fanning Factor shows exactly the same trend with Reynolds number under sCO₂ operating Temperature Variation. But, number of sample point reduces with the increase of sCO₂ pressure. The Colburn factor increases and the distribution profile becomes more well defined with operating pressure.

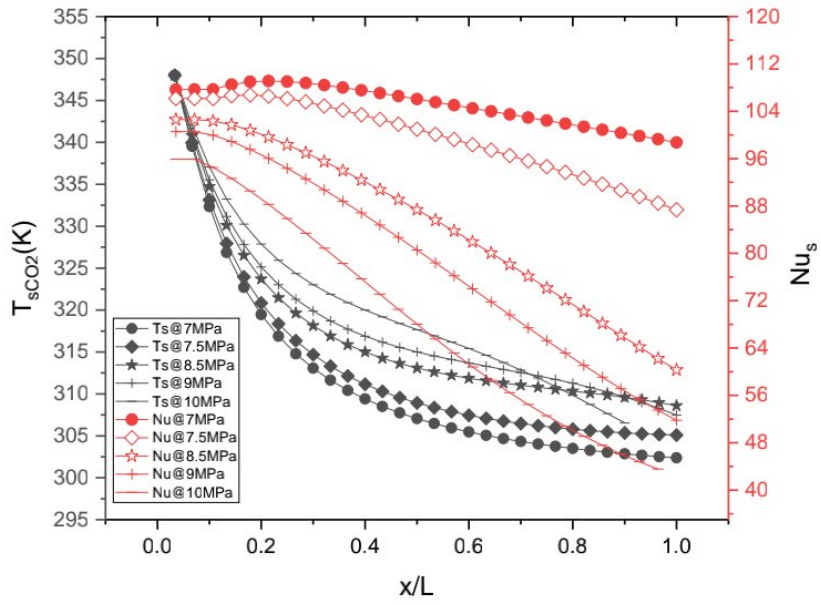


Figure 20: Temperature Profile and Dimensionless Temperature Profile across the length for different sCO₂ inlet pressure.

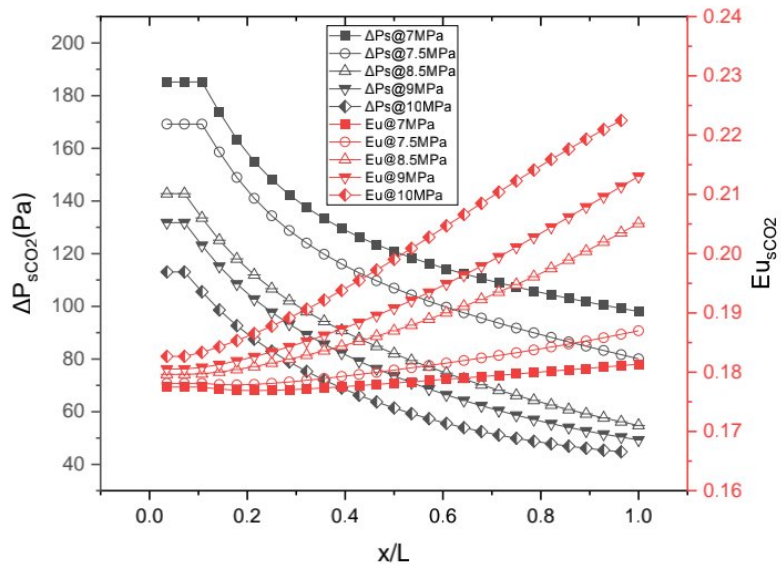


Figure 21: Influence of inlet sCO₂ Pressure on Pressure Drop characteristics of sCO₂

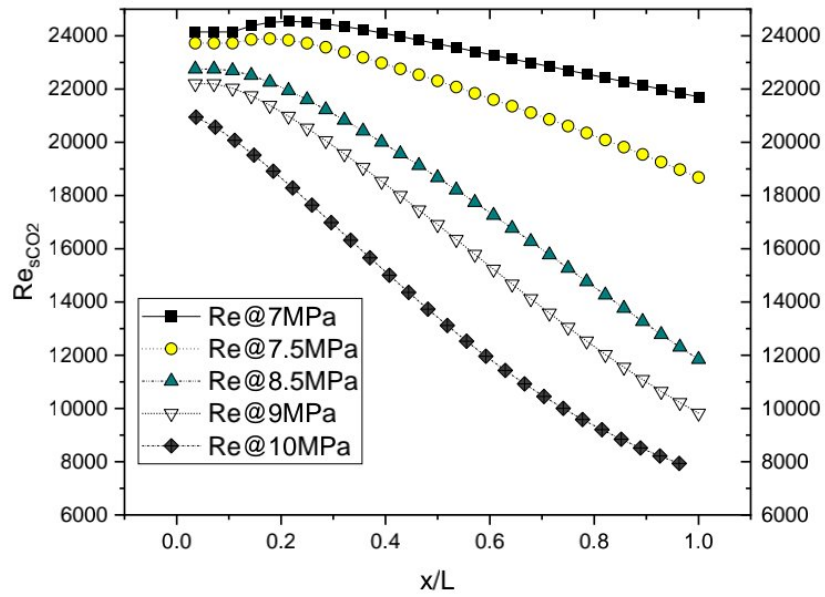


Figure 22: Reynolds Number distribution across the normalized length for different sCO_2 Pressure

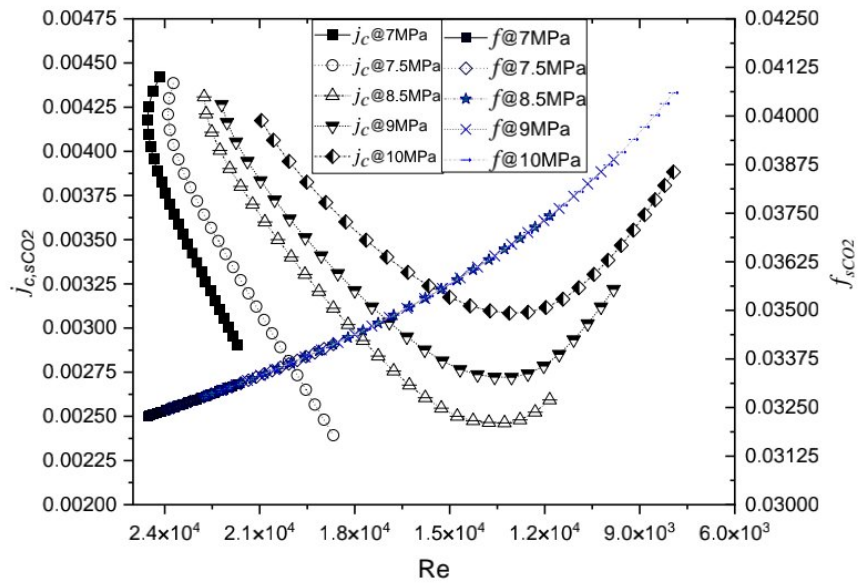


Figure 23: Influence of sCO_2 inlet pressure Thermohydraulic characteristics of sCO_2

4.4.2 Effect of Water Inlet Temperature

The effect of inlet temperature of Water as the coolant on the Temperature profiles across the normalized length is depicted in Figure 24. The inlet temperature was considered 348 K and the pre-cooler pressure was set 8 MPa. The temperature profiles for each fluid shows the similar trend when the water inlet temperature is 295.41K, 297.97K, 300.38K respectively. But The heat rejection rate requirement may not be fulfilled for above-mentioned cases. Also, the water inlet temperature may be higher than 300K during summer season due to high ambient air temperature as water itself is being cooled by the atmospheric air in a NDDCT (Ehsan, Duniam, Guan, et al. 2019). In those cases, the pumping power requirement will be higher as the mass flow rate of water required is more.

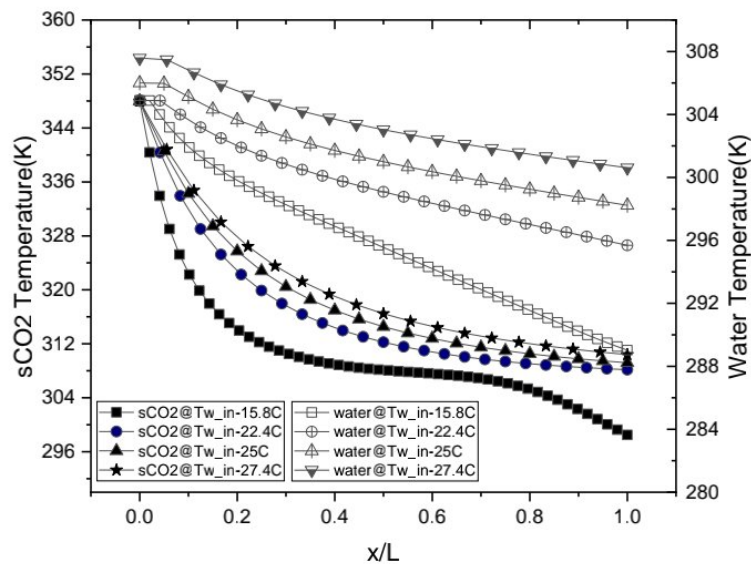


Figure 24: Effect of water inlet condition on Temperature Profiles across the normalized length

The Temperature profiles becomes steeper when the water inlet Temperature is 288.8K since the heat rejection happened to be the highest. As a result, the sCO2 outlet temperature becomes 298.5K.

However, the outlet temperature should not be less the pseudo-critical temperature to keep the cycle in Super critical region. If the pre-cooler outlet temperature reaches below 306.13K the cycle will enter the sub-critical region which is undesirable. In such cases the water mass flow rate must be reduced to halt the overcompensation of sCO₂ outlet temperature.

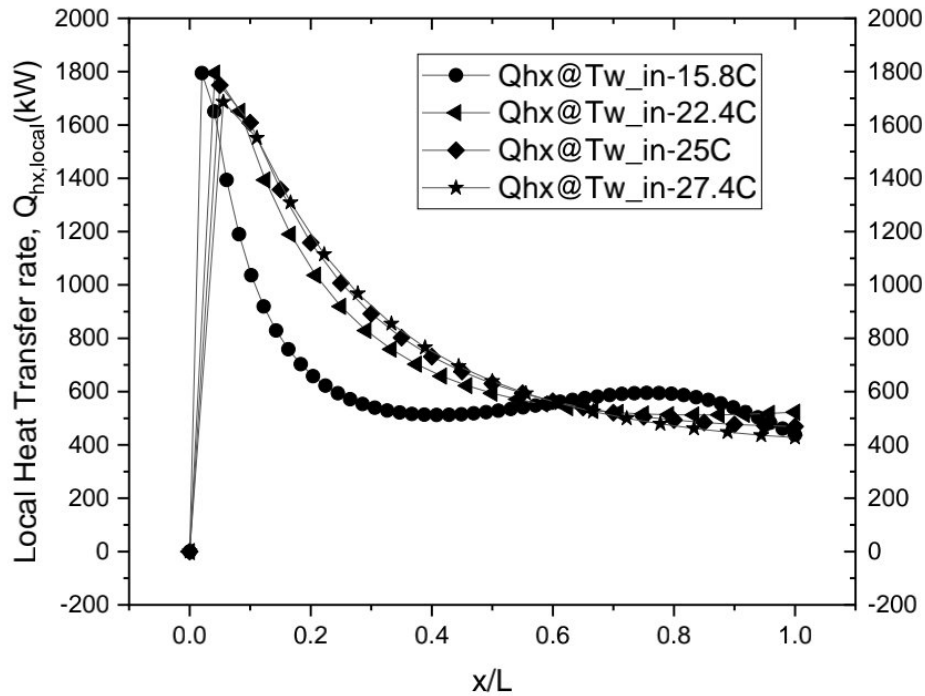


Figure 25: Effect of water inlet condition on local Heat Transfer rate

Figure 25, demonstrates the sectional heat exchanger capacity along the normalized length at different water inlet Temperature. The profile for the heat transfer rate shows similar trend for water inlet temperature above 283K.

However, the number of sections is being reduced in order to cope up with the pinch point phenomenon. The heat transfer rate shows a gradual rise at the 80% of the length of the Heat Exchanger. The maximum heat transfer rate remains around 1.8MW for each case.

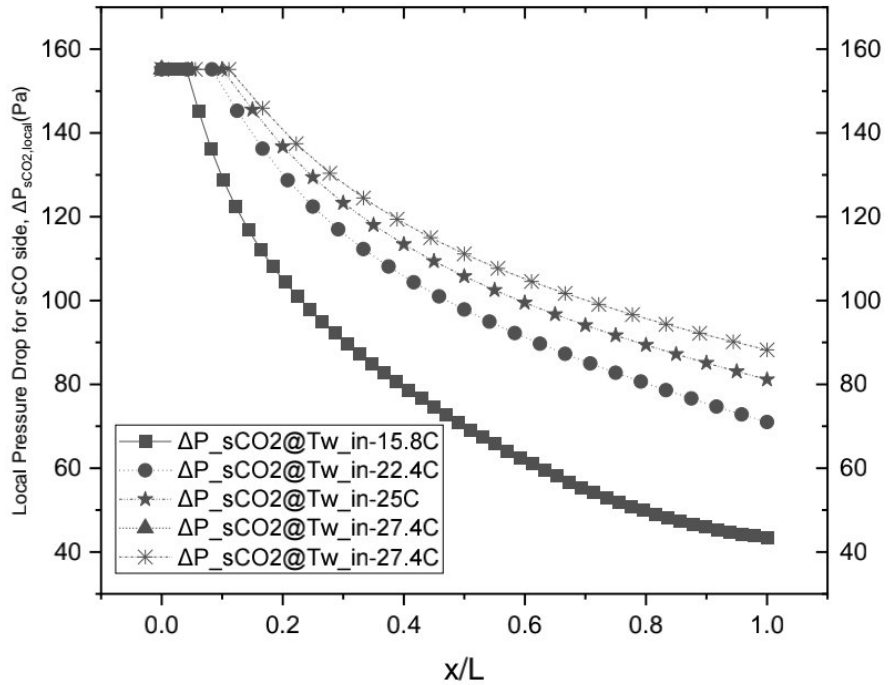


Figure 26: Local Pressure Drop characteristics along the normalized length at different water inlet temperatures

The pressure drop profiles indicates the lower inlet temperature will result steeper pressure drop profile but declined sectional pressure drop on the sCO2 side of the fluid, as shown in Figure 26. However, maximum sectional pressure drop remains at 158Pa.

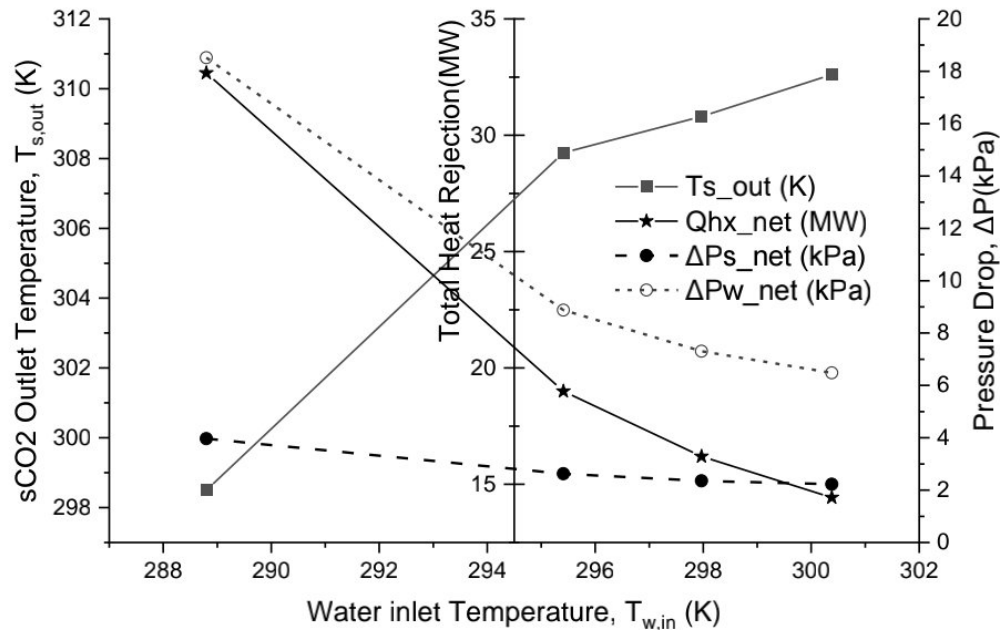


Figure 27:(a) sCO₂ outlet temperature, (b) Total heat transfer rate for the pre-cooler, (c) Total pressure drop characteristics with respect to the water inlet Temperature

The influence of different water inlet temperature on the sCO₂ outlet temperature, overall heat rejection as well as net pressure drop on both fluids has been summarized in Figure 27 under the inlet operating condition of 348K and 8MPa for sCO₂.

The heat transfer rate for pre-cooler is considerably affected by the variation of water inlet temperature. The total theoretical heat rejection by the pre-cooler is 32.67 MW for 288.38K on the other hand the heat rejection declines to only 14.43 MW for water inlet temperature of 300.38 K.

The mean outlet temperature of sCO₂ increases with the increase of water inlet temperature. The dereliction of reaching the outlet temperature to pseudo-critical temperature has some adverse effect on pre-cooler performance.

As a result, the sCO₂ will not reach to its highest density, if, the temperature does not reach the pseudo critical region at the pre-cooler pressure which will increase the requirement of Compressor power consumption.

However, the water inlet temperature has a little effect on sCO₂ net pressure drop. The water pressure reduces with the increase of water inlet temperature.

5 CHAPTER-FIVE CONCLUSION AND RECOMMENDATION

In this study, the in-house validated Python code an iterative nodal approach is implemented to a zigzag channel PCHE for the pre-cooler application of a sCO₂ recompression cycle integrated with CSP. The fluctuations of sCO₂ properties near the critical region plays an important role in designing the pre-cooler. This study also estimates the pre-cooler performance under the off-design application of the pre-cooler. Because sCO₂ has better heat transmission capabilities than water, the temperature profile for sCO₂ is steeper. The sCO₂ pressure distribution is convex, whereas the water pressure distribution is concave. On the water side, the net pressure loss is greater. The increased sCO₂ operating pressure raises the sCO₂ output temperature. The predicted exit temperature of sCO₂ is 302K at 7MPa operating pressure and 308.59K at 8.5MPa operating pressure. The pressure drop profiles show that the lower the input temperature, the steeper the pressure drop profile but the smaller the sectional pressure drop on the sCO₂ side of the fluid. The highest sectional pressure decrease, however, stays at 158Pa. The mean sCO₂ outflow temperature rises as the water intake temperature rises. If the temperature does not reach the pseudo critical area at the pre-cooler pressure, the sCO₂ will not achieve its maximum density, increasing the demand of Compressor work.

6 REFERENCES

- Baik, Seungjoon, Seong Gu Kim, Jekyoung Lee, and Jeong Ik Lee. 2017. "Study on CO₂ – Water Printed Circuit Heat Exchanger Performance Operating under Various CO₂ Phases for S-CO₂ Power Cycle Application." *Applied Thermal Engineering* 113: 1536–46. <https://doi.org/10.1016/j.applthermaleng.2016.11.132>.
- Bell, Ian H., Jorrit Wronski, Sylvain Quoilin, and Vincent Lemort. 2014. "Pure and Pseudo-Pure Fluid Thermophysical Property Evaluation and the Open-Source Thermophysical Property Library Coolprop." *Industrial and Engineering Chemistry Research* 53 (6): 2498–2508. <https://doi.org/10.1021/IE4033999>.
- Bennett, Katrine, and Yi tung Chen. 2019. "Printed Circuit Heat Exchanger Performance Analysis Using Non-Uniform Segmental Design Method." *Applied Thermal Engineering* 153 (February): 69–84. <https://doi.org/10.1016/j.applthermaleng.2019.02.102>.
- Bianchi, G, S S Saravi, R Loeb, K M Tsamos, M Marchionni, A Leroux, and S.A. n.d. "Tas-Sou, Design of a High-Temperature Heat to Power Conversion Facility for Testing Supercritical CO₂ Equipment and Packaged Power Units." *Energy Procedia* 161: 421–

- 428,. <https://doi.org/10.1016/j.egypro.2019.02.109>.
- Brun, Klaus, Peter Friedman, and Richard Dennis. 2017. *Fundamentals and Applications of Supercritical Carbon Dioxide (SCO₂) Based Power Cycles*. Woodhead publishing.
- Chen, Minghui, Xiaodong Sun, and Richard N. Christensen. 2019. "Thermal-Hydraulic Performance of Printed Circuit Heat Exchangers with Zigzag Flow Channels." *International Journal of Heat and Mass Transfer* 130: 356–67. <https://doi.org/10.1016/j.ijheatmasstransfer.2018.10.031>.
- Cheng, Keyong, Jingzhi Zhou, Huzhong Zhang, Xiulan Huai, and Jiangfeng Guo. 2020. "Experimental Investigation of Thermal-Hydraulic Characteristics of a Printed Circuit Heat Exchanger Used as a Pre-Cooler for the Supercritical CO₂ Brayton Cycle." *Applied Thermal Engineering* 171 (February): 115116. <https://doi.org/10.1016/j.applthermaleng.2020.115116>.
- Chu, Wen xiao, Xiong hui Li, Ting Ma, Yi tung Chen, and Qiu wang Wang. 2017. "Experimental Investigation on SCO₂-Water Heat Transfer Characteristics in a Printed Circuit Heat Exchanger with Straight Channels." *International Journal of Heat and Mass Transfer* 113: 184–94. <https://doi.org/10.1016/j.ijheatmasstransfer.2017.05.059>.
- Commission, European. n.d. "Summary for Policymakers." In *Climate Change 2013 - The Physical Science Basis*, edited by Intergovernmental Panel on Climate Change, 1–30. Cambridge: Cambridge University Press. <https://doi.org/10.1017/CBO9781107415324.004>.
- Dostal, Vaclav. 2004. "A Super c Ritical Carbon Dioxide Cycle."
- Ehsan, M. Monjurul, Sam Duniam, Zhiqiang Guan, Hal Gurgenci, and Alexander Klimenko. 2019. "Seasonal Variation on the Performance of the Dry Cooled Supercritical CO₂ Recompression Cycle." *Energy Conversion and Management* 197 (July): 111865. <https://doi.org/10.1016/j.enconman.2019.111865>.
- Ehsan, M. Monjurul, Sam Duniam, Jishun Li, Zhiqiang Guan, Hal Gurgenci, and Alexander Klimenko. 2019. "Effect of Cooling System Design on the Performance of the Recompression CO₂ Cycle for Concentrated Solar Power Application." *Energy* 180: 480–94. <https://doi.org/10.1016/j.energy.2019.05.108>.
- Ehsan, M. Monjurul, Zhiqiang Guan, and A. Y. Klimenko. 2018. "A Comprehensive Review on Heat Transfer and Pressure Drop Characteristics and Correlations with Supercritical CO₂ under Heating and Cooling Applications." *Renewable and Sustainable Energy Reviews* 92 (November 2017): 658–75. <https://doi.org/10.1016/j.rser.2018.04.106>.
- Foumeny, E. A., and P. J. Heggs. 1991. "Heat Exchange Engineering Volume 2," 385–97. https://books.google.com/books/about/Heat_Exchange_Engineering_Compact_heat_e.html?id=gwJUAAAAMAAJ.
- Guo, Jiangfeng, and Xiulan Huai. 2017. "Performance Analysis of Printed Circuit Heat Exchanger for Supercritical Carbon Dioxide." *Journal of Heat Transfer* 139 (6): 1–9. <https://doi.org/10.1115/1.4035603>.
- Gupta, Raghvendra, Paul E. Geyer, David F. Fletcher, and Brian S. Haynes. 2008. "Thermohydraulic Performance of a Periodic Trapezoidal Channel with a Triangular Cross-Section." *International Journal of Heat and Mass Transfer* 51 (11–12): 2925–29.

- <https://doi.org/10.1016/j.ijheatmasstransfer.2007.09.017>.
- H.I.H. Saravanamuttoo, H. Cohen, G. F. C. Rogers, and P. V. Straznicky A.C. Nix. 2017. "Gas Turbine Theory SEVENTH EDITION Gas Turbine Theory," 606.
- Herranz, L. E., J. I. Linares, and B. Y. Moratilla. 2009. "Power Cycle Assessment of Nuclear High Temperature Gas-Cooled Reactors." *Applied Thermal Engineering* 29 (8–9): 1759–65. <https://doi.org/10.1016/J.APPLTHERMALENG.2008.08.006>.
- Huang, Changye, Weihua Cai, Yue Wang, Yao Liu, Qian Li, and Biao Li. 2019. "Review on the Characteristics of Flow and Heat Transfer in Printed Circuit Heat Exchangers." *Applied Thermal Engineering* 153 (February): 190–205. <https://doi.org/10.1016/j.applthermaleng.2019.02.131>.
- I.R.E.N.A. n.d. "Global Renewables Outlook: Energy Transformation 2050."
- Ishizuka, Takao, Yasuyoshi Kato, Yasushi Muto, Konstantin Nikitin, Ngo Lam Tri, and Hiroyuki Hashimoto. 2005. "Thermal–Hydraulic Characteristic of a Printed Circuit Heat Exchanger in a Supercritical CO₂ Loop." In *The 11th International Topical Meeting on Nuclear Reactor Thermal–Hydraulics (NURETH-11)*. <https://cir.nii.ac.jp/crid/1571698600705529472.bib?lang=en>.
- Ji, Hwan Jeong, Sung Kim Lae, Keun Lee Jae, Yeong Ha Man, Soon Kim Kui, and Cheol Ahn Young. 2009. "Review of Heat Exchanger Studies for High-Efficiency Gas Turbines." *Proceedings of the ASME Turbo Expo 4 PART B* (March): 833–40. <https://doi.org/10.1115/GT2007-28071>.
- Johnston, By A M, W Levy, and S O Rumbold. 2001. "Application of Printed Circuit Heat Exchanger Technology within Heterogeneous Catalytic Reactors," no. November.
- Katz, Alon, Shaun R. Aakre, Mark H. Anderson, and Devesh Ranjan. 2021. "Experimental Investigation of Pressure Drop and Heat Transfer in High Temperature Supercritical CO₂ and Helium in a Printed-Circuit Heat Exchanger." *International Journal of Heat and Mass Transfer* 171: 121089. <https://doi.org/10.1016/j.ijheatmasstransfer.2021.121089>.
- Ke, Hanbing, Qi Xiao, Yiping Cao, Ting Ma, Yuansheng Lin, Min Zeng, and Qiuwang Wang. 2017. "Simulation of the Printed Circuit Heat Exchanger for S-CO₂ by Segmented Methods." *Energy Procedia* 142: 4098–4103. <https://doi.org/10.1016/j.egypro.2017.12.331>.
- Kim, Seong Gu, Youho Lee, Yoonhan Ahn, and Jeong Ik Lee. 2016. "CFD Aided Approach to Design Printed Circuit Heat Exchangers for Supercritical CO₂ Brayton Cycle Application." *Annals of Nuclear Energy* 92: 175–85. <https://doi.org/10.1016/j.anucene.2016.01.019>.
- Kim, Tae Ho, Jin Gyu Kwon, Sung Ho Yoon, Hyun Sun Park, Moo Hwan Kim, and Jae Eun Cha. 2015. "Numerical Analysis of Air-Foil Shaped Fin Performance in Printed Circuit Heat Exchanger in a Supercritical Carbon Dioxide Power Cycle." *Nuclear Engineering and Design* 288: 110–18. <https://doi.org/10.1016/j.nucengdes.2015.03.013>.
- Kim, Woojin, Young Jin Baik, Sangwoo Jeon, Daechan Jeon, and Chan Byon. 2017. "A Mathematical Correlation for Predicting the Thermal Performance of Cross, Parallel, and Counterflow PCHEs." *International Journal of Heat and Mass Transfer* 106: 1294–

1302. <https://doi.org/10.1016/j.ijheatmasstransfer.2016.10.110>.
- Kim, Y W, J H Kang, and E S Kim. 2018. "Mechanical Design for Key Dimensions of Printed Circuit Heat Exchanger." *Transactions of the Korean Nuclear Society Spring Meeting*. https://www.kns.org/files/pre_paper/39/18S-069김용환.pdf.
- Lao, Jiewei, Jing Ding, Qianmei Fu, Weilong Wang, and Jianfeng Lu. 2019. "Heat Transfer between Molten Salt and Supercritical CO₂ in Discontinuous Fins Print Circuits Heat Exchanger." *Energy Procedia* 158 (February): 5832–37. <https://doi.org/10.1016/J.EGYPRO.2019.01.544>.
- Lee, Sang Moon, and Kwang Yong Kim. 2013. "Comparative Study on Performance of a Zigzag Printed Circuit Heat Exchanger with Various Channel Shapes and Configurations." *Heat and Mass Transfer/Waerme- Und Stoffuebertragung* 49 (7): 1021–28. <https://doi.org/10.1007/s00231-013-1149-4>.
- Li, Ming Jia, Han Hui Zhu, Jia Qi Guo, Kun Wang, and Wen Quan Tao. 2017. "The Development Technology and Applications of Supercritical CO₂ Power Cycle in Nuclear Energy, Solar Energy and Other Energy Industries." *Applied Thermal Engineering* 126: 255–75. <https://doi.org/10.1016/j.applthermaleng.2017.07.173>.
- Li, Qi, Gilles Flamant, Xigang Yuan, Pierre Neveu, and Lingai Luo. 2011. "Compact Heat Exchangers: A Review and Future Applications for a New Generation of High Temperature Solar Receivers." *Renewable and Sustainable Energy Reviews* 15 (9): 4855–75. <https://doi.org/10.1016/j.rser.2011.07.066>.
- Li, Xiong hui, Tian rui Deng, Ting Ma, Han bing Ke, and Qiu wang Wang. 2019a. "A New Evaluation Method for Overall Heat Transfer Performance of Supercritical Carbon Dioxide in a Printed Circuit Heat Exchanger." *Energy Conversion and Management* 193: 99–105. <https://doi.org/10.1016/j.enconman.2019.04.061>.
- . 2019b. "A New Evaluation Method for Overall Heat Transfer Performance of Supercritical Carbon Dioxide in a Printed Circuit Heat Exchanger." *Energy Conversion and Management* 193 (April): 99–105. <https://doi.org/10.1016/j.enconman.2019.04.061>.
- Linares, José I., María J. Montes, Alexis Cantizano, and Consuelo Sánchez. 2020. "A Novel Supercritical CO₂ Recompression Brayton Power Cycle for Power Tower Concentrating Solar Plants." *Applied Energy* 263 (February): 114644. <https://doi.org/10.1016/j.apenergy.2020.114644>.
- Liu, Sheng hui, Yan ping Huang, Jun feng Wang, Rui long Liu, and Jin guang Zang. 2020. "Experimental Study of Thermal-Hydraulic Performance of a Printed Circuit Heat Exchanger with Straight Channels." *International Journal of Heat and Mass Transfer* 160: 120109. <https://doi.org/10.1016/j.ijheatmasstransfer.2020.120109>.
- Luu, M T, D Milani, R McNaughton, and A Abbas. n.d. "Dynamic Modelling and Start-up Operation of a Solar-Assisted Recompression Supercritical CO₂ Brayton Power Cycle." *Appl. Energy* 199: 247–263.
- Marchionni, M, G Bianchi, and S A Tassou. n.d. "Transient Analysis and Control of a Heat to Power Conversion Unit Based on a Simple Regenerative Supercritical CO₂ Joule-Brayton Cycle." *Appl. Therm. Eng* 183: 116214.
- Milani, Dia, Minh Tri Luu, Robbie McNaughton, and Ali Abbas. 2017. "Optimizing an

- Advanced Hybrid of Solar-Assisted Supercritical CO₂ Brayton Cycle: A Vital Transition for Low-Carbon Power Generation Industry.” *Energy Conversion and Management* 148: 1317–31. <https://doi.org/10.1016/j.enconman.2017.06.017>.
- Moore, Robert Charles, Nathan Phillip Siegel, Gregory J Kolb, Milton E Vernon, and Clifford Kuofei Ho. 2010. “Design Considerations for Concentrating Solar Power Tower Systems Employing Molten Salt.” September. <https://doi.org/10.2172/1008140>.
- Ngo, Tri Lam, Yasuyoshi Kato, Konstantin Nikitin, and Takao Ishizuka. 2007. “Heat Transfer and Pressure Drop Correlations of Microchannel Heat Exchangers with S-Shaped and Zigzag Fins for Carbon Dioxide Cycles.” *Experimental Thermal and Fluid Science* 32 (2): 560–70. <https://doi.org/10.1016/j.expthermflusci.2007.06.006>.
- Ngo, Tri Lam, Yasuyoshi Kato, Konstantin Nikitin, and Nobuyoshi Tsuzuki. 2006. “New Printed Circuit Heat Exchanger with S-Shaped Fins for Hot Water Supplier.” *Experimental Thermal and Fluid Science* 30 (8): 811–19. <https://doi.org/10.1016/j.expthermflusci.2006.03.010>.
- Nikitin, Konstantin, Yasuyoshi Kato, and Takao Ishizuka. 2007. “Icone15-10826 Experimental Thermal-Hydraulics Comparison of Microchannel Heat Exchangers With Zigzag Channels and S-Shaped Fins for Gas Turbine Reactors.” *The Proceedings of the International Conference on Nuclear Engineering (ICONE) 2007*.15 (0): _ICONE1510- _ICONE1510. https://doi.org/10.1299/jsmeicone.2007.15._icone1510_427.
- Nikitin, Konstantin, Yasuyoshi Kato, and Lam Ngo. 2006. “Printed Circuit Heat Exchanger Thermal-Hydraulic Performance in Supercritical CO₂ Experimental Loop.” *International Journal of Refrigeration* 29 (5): 807–14. <https://doi.org/10.1016/j.ijrefrig.2005.11.005>.
- Park, J H, J Yoon, J Eoh, H Kim, and M H Kim. n.d. “Optimization and Sensitivity Analysis of the Nitrogen Brayton Cycle as a Power Conversion System for a Sodium– Cooled Fast Reactor, Nucl.” *Eng. Des* 340: 325–334.
- Park, Joo Hyun, Jin Gyu Kwon, Tae Ho Kim, Moo Hwan Kim, Jae Eun Cha, and Hang Jin Jo. 2020. “Experimental Study of a Straight Channel Printed Circuit Heat Exchanger on Supercritical CO₂ near the Critical Point with Water Cooling.” *International Journal of Heat and Mass Transfer* 150. <https://doi.org/10.1016/j.ijheatmasstransfer.2020.119364>.
- Park, S, J Kim, M Yoon, D Rhim, and C Yeom. n.d. “Thermodynamic and Economic Investigation of Coal-Fired Power Plant Combined with Various Supercritical CO₂ Brayton Power Cycle.” *Appl. Therm. Eng* 130: 611–623.
- Pérez-Pichel, G. D., J. I. Linares, L. E. Herranz, and B. Y. Moratilla. 2012. “Thermal Analysis of Supercritical CO₂ Power Cycles: Assessment of Their Suitability to the Forthcoming Sodium Fast Reactors.” *Nuclear Engineering and Design* 250 (September): 23–34. <https://doi.org/10.1016/J.NUCENGDDES.2012.05.011>.
- Pierres, Renaud Le, David Southall, and Stephen Osborne. 2011. “Impact of Mechanical Design Issues on Printed Circuit Heat Exchangers.” *Proceedings of SCO₂ Power Cycle Symposium*, 24–25.
- “Printed Circuit Heat Exchangers - Meggitt.” n.d. Accessed May 16, 2022. <https://www.meggitt.com/products-services/printed-circuit-heat-exchangers/>.

- Ren, Zhuo, Chen Ru Zhao, Pei Xue Jiang, and Han Liang Bo. 2019. "Investigation on Local Convection Heat Transfer of Supercritical CO₂ during Cooling in Horizontal Semicircular Channels of Printed Circuit Heat Exchanger." *Applied Thermal Engineering* 157 (November 2018): 113697. <https://doi.org/10.1016/j.applthermaleng.2019.04.107>.
- Sabharwall, Piyush, Denis Clark, Michael Glazoff, Guiqiu Zheng, Kumar Sridharan, and Mark Anderson. 2014. "Advanced Heat Exchanger Development for Molten Salts." *Nuclear Engineering and Design* 280 (December): 42–56. <https://doi.org/10.1016/J.NUCENGDES.2014.09.026>.
- Saeed, Muhammad, Abdallah S. Berrouk, M. Salman Siddiqui, and Ahmad Ali Awais. 2020. "Numerical Investigation of Thermal and Hydraulic Characteristics of SCO₂-Water Printed Circuit Heat Exchangers with Zigzag Channels." *Energy Conversion and Management* 224 (June): 113375. <https://doi.org/10.1016/j.enconman.2020.113375>.
- Saeed, Muhammad, and Man Hoe Kim. 2017. "Thermal and Hydraulic Performance of SCO₂ PCHE with Different Fin Configurations." *Applied Thermal Engineering* 127: 975–85. <https://doi.org/10.1016/j.applthermaleng.2017.08.113>.
- . 2019. "Thermal-Hydraulic Analysis of Sinusoidal Fin-Based Printed Circuit Heat Exchangers for Supercritical CO₂ Brayton Cycle." *Energy Conversion and Management* 193 (April): 124–39. <https://doi.org/10.1016/j.enconman.2019.04.058>.
- Saeed, Muhammed, Ahmad Ali Awais, and Abdallah S. Berrouk. 2021. "CFD Aided Design and Analysis of a Precooler with Zigzag Channels for Supercritical CO₂ Power Cycle." *Energy Conversion and Management* 236: 114029. <https://doi.org/10.1016/j.enconman.2021.114029>.
- Saeed, Muhammed, Abdallah S. Berrouk, M. Salman Siddiqui, and Ahmad Ali Awais. 2020. "Effect of Printed Circuit Heat Exchanger's Different Designs on the Performance of Supercritical Carbon Dioxide Brayton Cycle." *Applied Thermal Engineering* 179 (February): 115758. <https://doi.org/10.1016/j.applthermaleng.2020.115758>.
- Shah, Ramesh K., and Duan P. Sekuli. 2003. *Fundamentals of Heat Exchanger Design. Introduction to Thermo-Fluids Systems Design*. Hoboken, NJ, USA: John Wiley & Sons, Inc. <https://doi.org/10.1002/9780470172605>.
- Song, J, X Li, K Wang, and C N Markides. n.d. "Parametric Optimisation of a Combined Supercritical CO₂ (s-CO₂) Cycle and Organic Rankine Cycle (ORC) System for Internal Combustion Engine (ICE) Waste-Heat Recovery, Energy Convers." *Manag* 218: 112999.
- The American Society of Mechanical Engineers (ASME). 2010. "Part D Properties (Customary)." In *ASME Boil. Press. Vessel CODE*. ASME International.
- . 2011. "Section 8 Div 1 - Rules for Construction of Pressure Vessels." In *ASME Boil. Press. Vessel CODE*. ASME International.
- Turchi, Craig S., Zhiwen Ma, Ty W. Neises, and Michael J. Wagner. 2013. "Thermodynamic Study of Advanced Supercritical Carbon Dioxide Power Cycles for Concentrating Solar Power Systems." *Journal of Solar Energy Engineering, Transactions of the ASME* 135 (4). <https://doi.org/10.1115/1.4024030>.

- Wang, Kun, Ming Jia Li, Jia Qi Guo, Peiwen Li, and Zhan Bin Liu. 2018. "A Systematic Comparison of Different S-CO₂ Brayton Cycle Layouts Based on Multi-Objective Optimization for Applications in Solar Power Tower Plants." *Applied Energy* 212 (December 2017): 109–21. <https://doi.org/10.1016/j.apenergy.2017.12.031>.
- Wang, Wen Qi, Yu Qiu, Ya Ling He, and Hong Yuan Shi. 2019. "Experimental Study on the Heat Transfer Performance of a Molten-Salt Printed Circuit Heat Exchanger with Airfoil Fins for Concentrating Solar Power." *International Journal of Heat and Mass Transfer* 135: 837–46. <https://doi.org/10.1016/j.ijheatmasstransfer.2019.02.012>.
- White, Martin T., Giuseppe Bianchi, Lei Chai, Savvas A. Tassou, and Abdulnaser I. Sayma. 2021. "Review of Supercritical CO₂ Technologies and Systems for Power Generation." *Applied Thermal Engineering* 185 (December 2020). <https://doi.org/10.1016/j.applthermaleng.2020.116447>.
- Wu, P, C Gao, Y Huang, D Zhang, and J Shan. n.d. "Supercritical CO₂ Brayton Cycle Design for Small Modular Reactor with a Thermodynamic Analysis Solver, Sci." *Technol. Nucl. Install.*
- Wu, Pan, Yunduo Ma, Chuntian Gao, Weihua Liu, Jianqiang Shan, Yanping Huang, Junfeng Wang, Dan Zhang, and Xu Ran. 2020. "A Review of Research and Development of Supercritical Carbon Dioxide Brayton Cycle Technology in Nuclear Engineering Applications." *Nuclear Engineering and Design* 368 (July): 110767. <https://doi.org/10.1016/j.nucengdes.2020.110767>.
- Yin, Jun Ming, Qiu Yun Zheng, Zhao Rui Peng, and Xin Rong Zhang. 2020. "Review of Supercritical CO₂ Power Cycles Integrated with CSP." *International Journal of Energy Research* 44 (3): 1337–69. <https://doi.org/10.1002/er.4909>.
- Yoon, Su Jong, James O'Brien, Minghui Chen, Piyush Sabharwall, and Xiaodong Sun. 2017. "Development and Validation of Nusselt Number and Friction Factor Correlations for Laminar Flow in Semi-Circular Zigzag Channel of Printed Circuit Heat Exchanger." *Applied Thermal Engineering* 123: 1327–44. <https://doi.org/10.1016/j.applthermaleng.2017.05.135>.
- Zhang, Haiyan, Jiangfeng Guo, Xiulan Huai, and Xinying Cui. 2019. "Thermodynamic Performance Analysis of Supercritical Pressure CO₂ in Tubes." *International Journal of Thermal Sciences* 146 (July): 106102. <https://doi.org/10.1016/j.ijthermalsci.2019.106102>.
- Zohuri, Bahman. 2016. *Compact Heat Exchangers: Selection, Application, Design and Evaluation*. *Compact Heat Exchangers: Selection, Application, Design and Evaluation*. <https://doi.org/10.1007/978-3-319-29835-1>.